Phononics in Low-Dimensional Materials: Engineering Phonon Spectrum

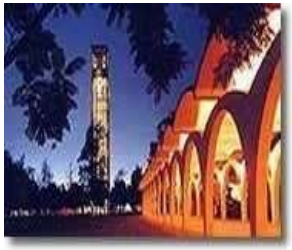

Alexander A. Balandin

Nano-Device Laboratory
Department of Electrical Engineering and
Materials Science and Engineering Program
University of California – Riverside

Bremen, Germany – Keynote Talk – 2013

NRI nanoelectronics RESEARCH INITIATIVE

FENA ONR Office of Naval Research NSF STARnet SRC DARPA FAME

| Nano-Device Laboratory >

UC RIVERSIDE
UNIVERSITY OF CALIFORNIA

City of Riverside


UCR Bell Tower


UCR Botanic Gardens


UCR Engineering Building


Joshua Tree Park, California

Nano-Device Laboratory (NDL)
Department of Electrical Engineering
University of California – Riverside

| Nano-Device Laboratory >

UNIVERSITY OF CALIFORNIA UC RIVERSIDE

Profile: experimental and theoretical research in advanced materials and nano-devices

PI: Alexander A. Balandin

Thermal and Electrical Characterization

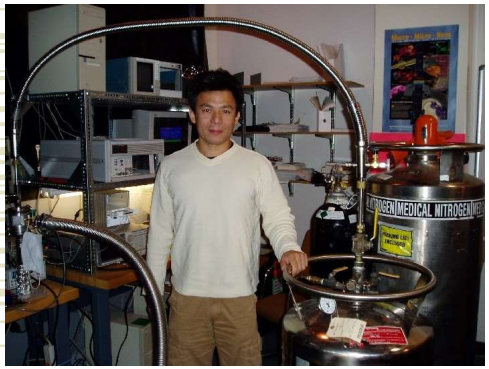

Phononics Research & Applications

Nanoscale Characterization

Electronic Devices and Circuits

Direct Energy Conversion

Optoelectronics

Bio-Nanotech

Theory and Modeling

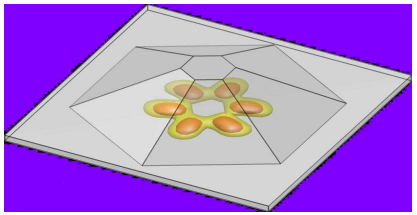

Device Design and Characterization

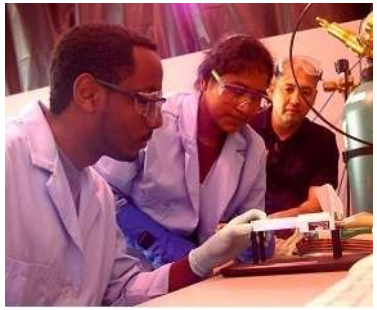

Raman, Fluorescence and PL Spectroscopy

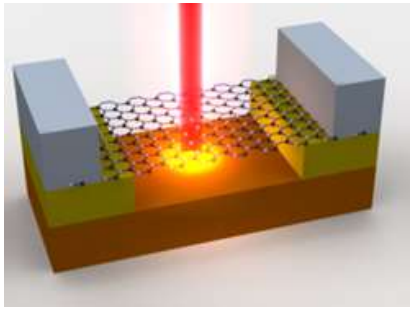

Outline

- *Part I: Overview of Phononics and Phonon Engineering*
- *Part II: Phonons in Graphene*
  - *Specifics of 2D phonon thermal transport*
  - *Engineering phonons by twisting atomic planes*
- *Part III: Phonons in van der Waals Materials*
  - *Restacking the layers*
  - *Charge-density waves*
- *Part IV: Applications of Phononics*
  - *Thermal interface materials*
  - *Heat spreaders*
  - *Thermoelectric energy generation*
  - *Low-power information processing*
- *Conclusions*

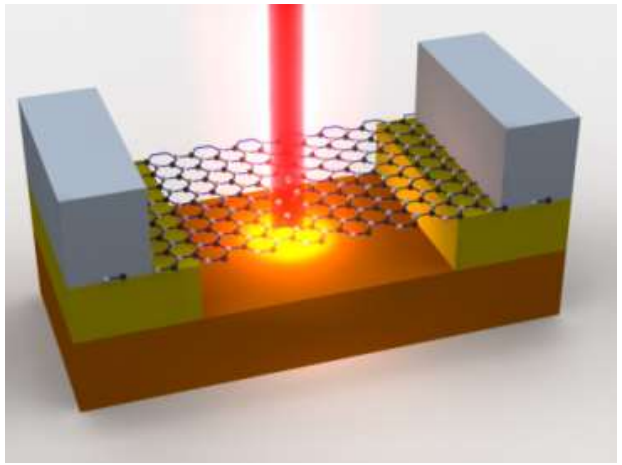

Part I: Overview of Phononics and Phonon Engineering

Cross sections of polar optical phonon modes with l = 3, 4 and for the spherical ZnO quantum dot. Blue and red colors denote negative and positive values of phonon potentials, correspondingly.

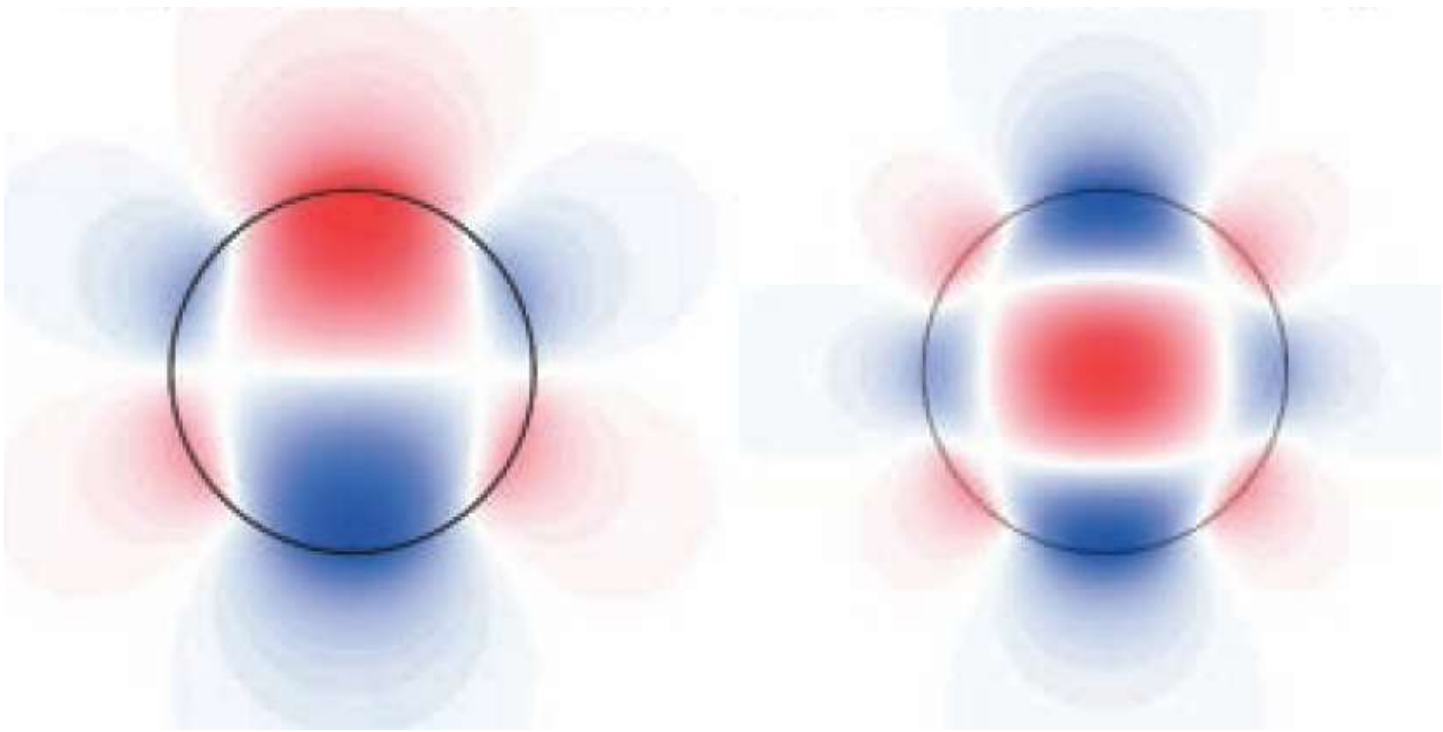

Alexander A. Balandin, University of California – Riverside

Phononics → Nanoscale Phonon Engineering

Definition: phonon engineering is an approach for modifying the thermal, electrical and optical properties of materials via tuning the phonon characteristics at nanometer scale through the spatial confinement-induced changes in the phonon spectrum.

Band-structure engineering: mismatch of E_G

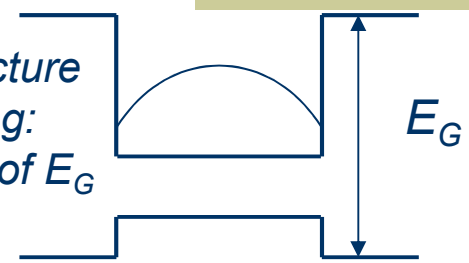

Goals:

Change in electron – phonon scattering → drift mobility

Change in phonon group velocity → thermal conductivity

Control of the phonon energies → optical response

Tuning Parameters:

Crystalline structure

Dimensions

Sound velocity

Mass density

Acoustic Impedance

Interface

Optical phonon frequencies

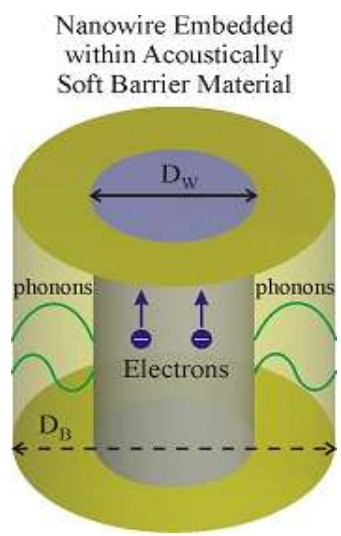

Phonon engineering: mismatch of $Z=\rho V_{sound}$

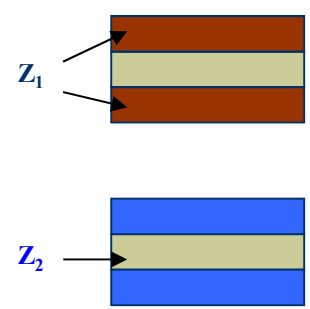

Acoustic Impedance: $Z=\rho V_s$ [kg/m^{2}s]

A.A. Balandin, "Nanophononics: Phonon engineering in nanostructures and nanodevices," *J. Nanoscience and Nanotechnology*, **5**, 7 (2005).

Rytov Model for Folded Phonons in Thinly Laminated Media

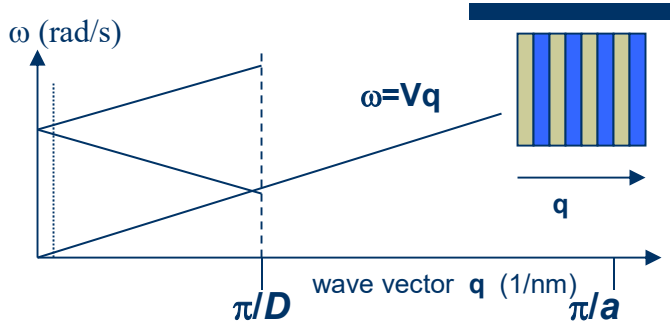

Rytov (1956) Model for Thinly Laminated Medium

$$\cos(qD) = \cos\left(\frac{\omega D_1}{V_1}\right)\cos\left(\frac{\omega D_2}{V_2}\right) - \frac{1+\varsigma^2}{2\varsigma}\sin\left(\frac{\omega D_1}{V_1}\right)\sin\left(\frac{\omega D_2}{V_2}\right),$$

V_i is the sound velocity in each layer, and $\zeta=\rho_2 V_2/\rho_1 V_1$ is the acoustic mismatch between the layers, $D=D_1+D_2$ is the period of the superlattice.

S. M. Rytov, *Soviet Physics - Acoustics*, **2**, 67 (1956).

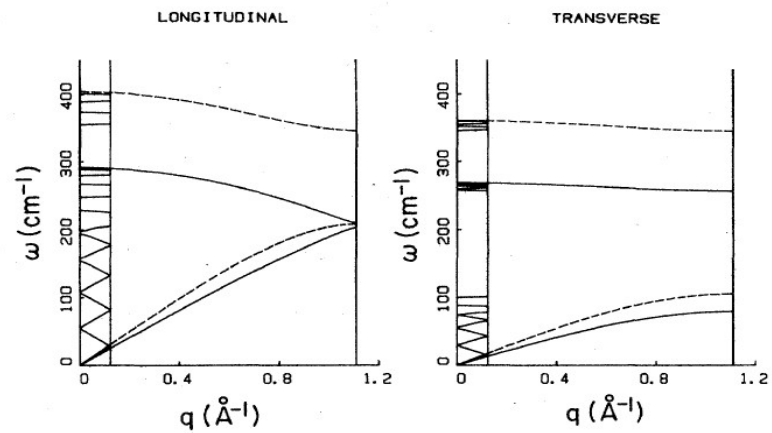

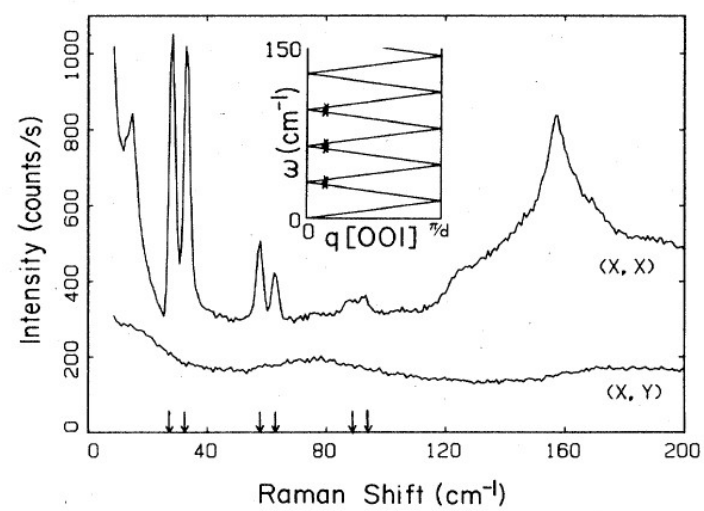

Raman spectrum of superlattice. Inset is Rytov-model calculations showing *q* of the folded LA peaks. The arrows indicate predicted peak frequencies corresponding to a superlattice period of 52 A.

The data is after C. Colvard et al., *Phys. Rev. B*, **31**, 2080 (1985)

Bulk vs. Confined Acoustic Phonons

Bulk Semiconductor

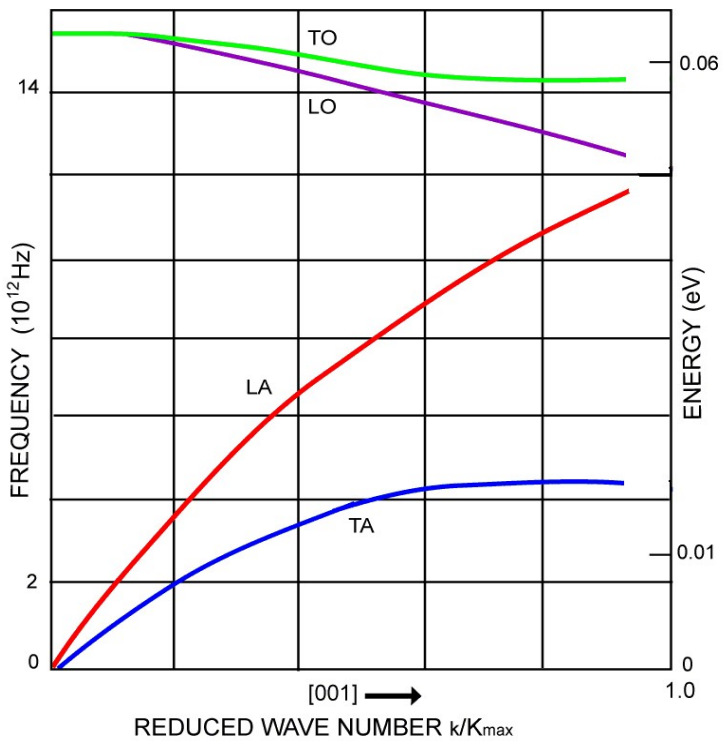

E.P. Pokatilov, D.L. Nika and A.A. Balandin, "Acoustic-phonon propagation in semiconductor nanowires with elastically dissimilar barriers," *Physical Review B*, **72**, 113311 (2005)

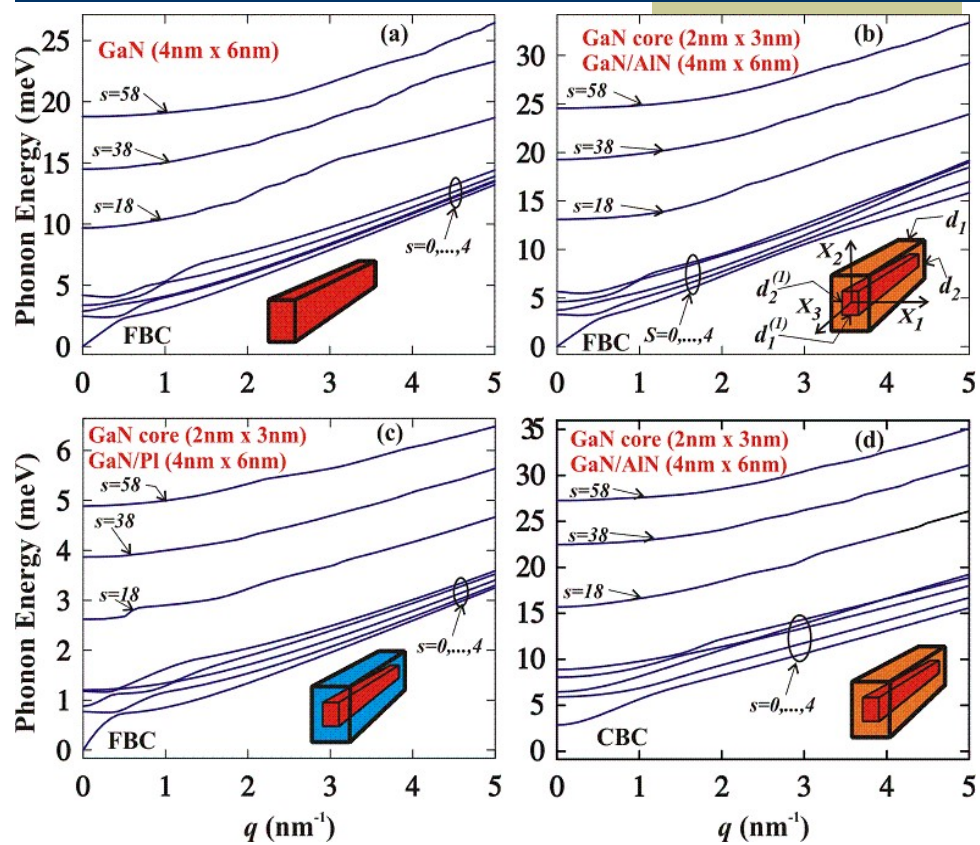

D.L. Nika, E.P. Pokatilov and A.A. Balandin, "Phonon - engineered mobility enhancement in the acoustically mismatched transistor channels," *Appl. Phys. Lett.*, **93**, 173111 (2008).

Thermal Conductivity of Nanostructures Beyond "Classical" Size Effects

"Classical" size effects on heat conduction: phonon – boundary scattering

Casimir (1938), Berman (1955), Ziman (1960)

Phonon – boundary scattering rate:

$$\frac{1}{\tau_B} = \zeta \frac{1-p}{1+p} \frac{<\upsilon>}{L}$$

PHYSICAL REVIEW B VOLUME 58, NUMBER 3 15 JULY 1998-I

Significant decrease of the lattice thermal conductivity due to phonon confinement in a free-standing semiconductor quantum well

Alexander Balandin and Kang L. Wang
Device Research Laboratory, Electrical Engineering Department, University of California–Los Angeles, Los Angeles, California 90095-1594

(Received 17 February 1998; revised manuscript received 20 April 1998)

Tuning thermal conductivity can be approached with appropriate modification of phonon modes, e.g., phonon engineering.

Thermal Conductivity of Nanowires: Boundary Size Effects

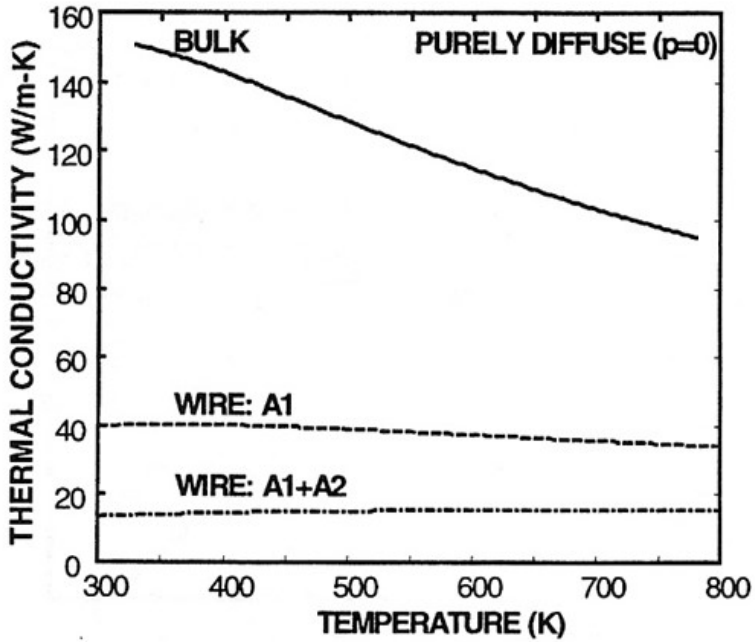

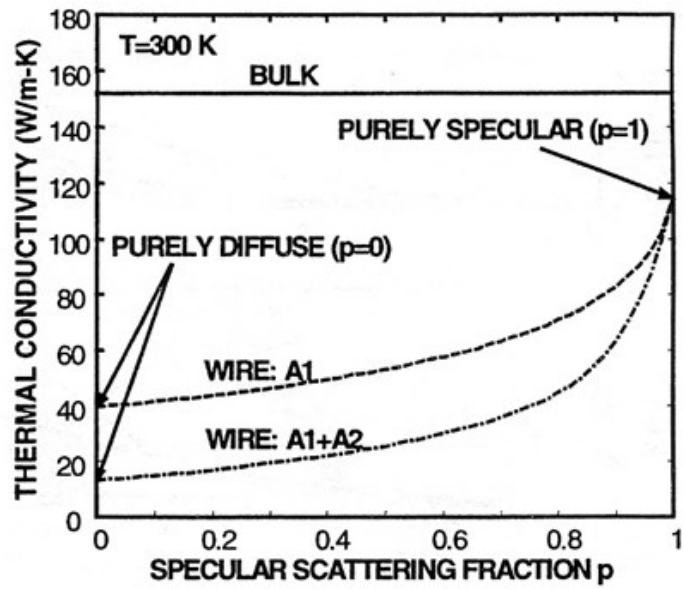

J. Zou and A. Balandin, Phonon heat conduction in a semiconductor nanowire, *J. Applied Physics*, **89**, 2932 (2001.)

→ Predicted decrease of the thermal conductivity from 148 W/m-K in bulk to about 13 W/m-K in 20 nm Si crystalline nanowire at T=300 K (2001).

→ Agreement with experimental study: ~ 9 W/m-K in 22 nm nanowire at T=300K; strong diameter dependence; deviation from Debye T^3 law at low T, Majumdar Group, UCB (2003).

Thermal Conductivity Inhibition in Phonon Engineered Nanowires

Models:
→ Five-parameter Born-von Karman
→ Six-parameter valence-force field

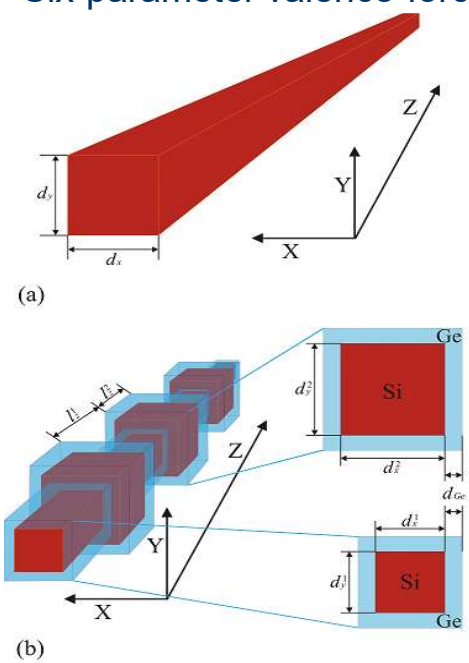

Details: D.L. Nika, A.I. Cocemasov, D.V. Crismari and A.A. Balandin, *Appl. Phys. Lett.*, **102**, 213109 (2013)

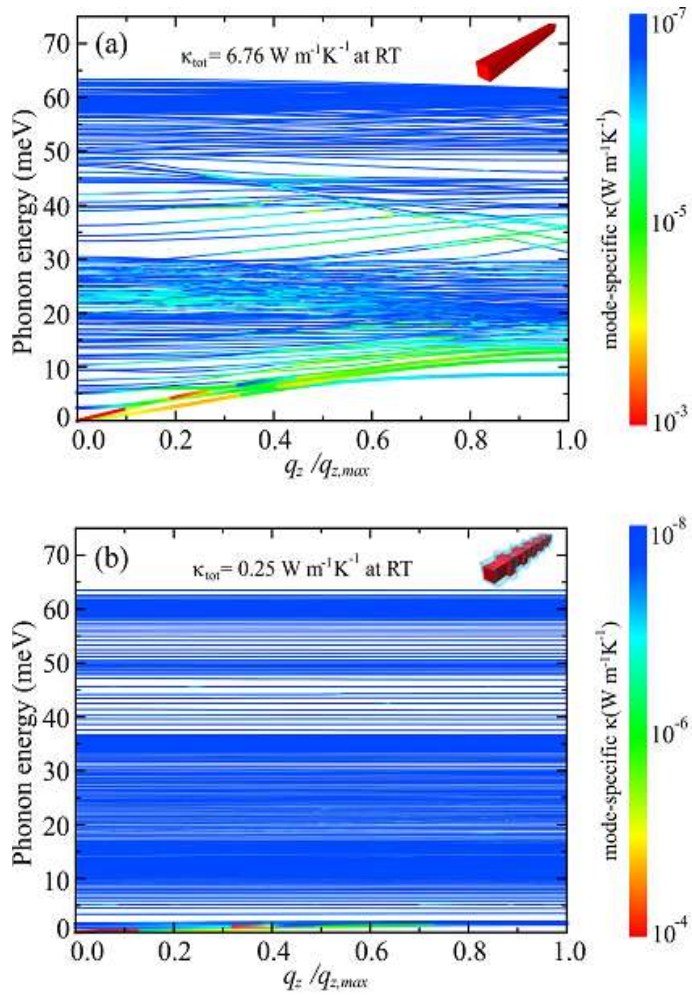

K of Si/Ge cross-section modulated nanowires is *three orders* of magnitude lower than that of bulk Si.

Thermal flux in the modulated nanowires is suppressed by an order of magnitude in comparison with generic Si nanowires.

Modification of phonon spectra in modulated nanowires leading to decrease of the phonon group velocities and localization of the certain phonon modes.

K inhibition is achieved in nanowires *without* additional surface roughness.

Electron Mobility in Nanowires: Effect of the Electron Confinement

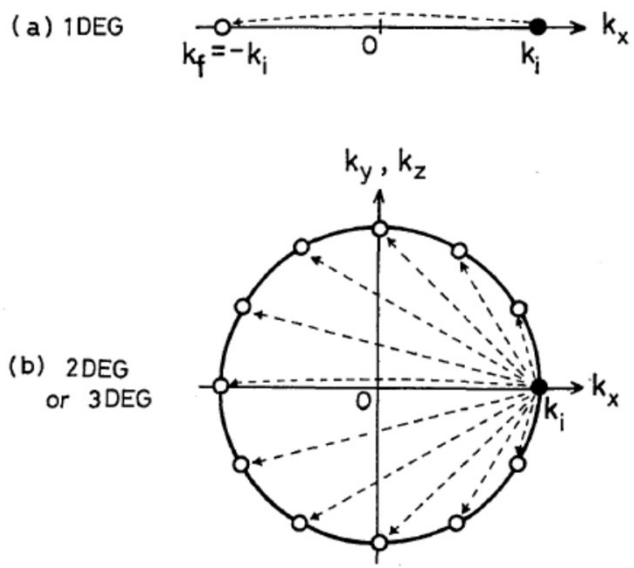

GaAs nanowire at low T

Assumptions:
confined electrons (infinite potential well)
remote ionized impurity scattering

Predictions: mobility increase > 10^6 cm^2/Vs

H. Sakaki, *Jap J. Appl. Phys.*, **19**, L735 (1980).

Results of J. Lee and M.O. Vassell, *J. Phys. C: Solid State Physics*, **17**, 2525 (1984).

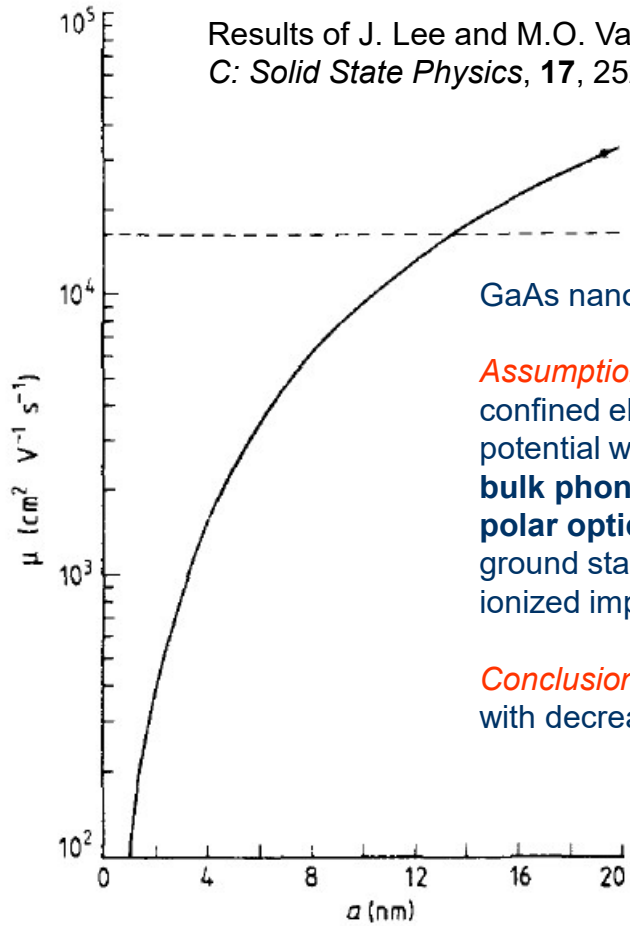

GaAs nanowire at T=200 K

Assumptions:
confined electrons (infinite potential well)
bulk phonons (acoustic and polar optical)
ground state sub-band only
ionized impurity scattering

Conclusions: $1/\tau_{ph}$ increases with decreasing ***a***

Mobility Calculation in Silicon Nanowires: Bulk vs. Confined Phonons

$$\mu_l \sim (m^*)^{-5/2} T^{-3/2}$$ ← acoustic phonons

$$\mu_i \sim (m^*)^{-1/2} N_I^{-1} T^{3/2}$$ ← ionized impurities

Momentum relaxation rate due to phonons:

$$\tau_{\mathrm{ph}}^{-1}(k_z) = \frac{2\pi}{\hbar} E_a^2 \sum_{\mathbf{q}} \left| \left\langle \nabla \cdot \mathbf{u}_{\mathbf{q}} \right\rangle \right|^2 \frac{q_z}{k_z} \left[\left(N_{\mathbf{q}} + 1 \right) \delta(\varepsilon_{k_z - q_z} + \hbar\omega_{\mathbf{q}} - \varepsilon_{k_z}) + N_{-\mathbf{q}} \delta(\varepsilon_{k_z - q_z} - \hbar\omega_{-\mathbf{q}} - \varepsilon_{k_z}) \right]$$

Momentum relaxation rate due to ionized impurities:

$$\tau_{\mathrm{imp}}^{-1}(k_z) = \frac{2\pi m N_I R_1^2}{\hbar^3 k_z} \left(\frac{Ze^2}{2\pi\varepsilon_0\varepsilon} \right)^2 \left[\ln(k_z R_1) \right]^2$$

The low-field electron mobility in the nanowire:

$$\mu = -2\frac{e}{m} \int_0^\infty \varepsilon^{1/2} \frac{\partial f_0}{\partial \varepsilon} \tau(\varepsilon) d\varepsilon \Big/ \int_0^\infty \varepsilon^{-1/2} f_0(\varepsilon) d\varepsilon$$

$f_o(\varepsilon)$ is the electron occupation number given by the Fermi-Dirac distribution. In the non-degenerate case, it is given by a Maxwellian distribution.

Phonons in a cylindrical nanowire:

$$\mathbf{u}_{\omega,q_z} = \left[\left(\frac{dG}{dr_\perp} + q_z \frac{dF}{dr_\perp} \right) \mathbf{e}_\rho + i\left(-q_z G(r_\perp) + q_t^2 F(r_\perp) \right) \mathbf{e}_z \right] e^{-iq_z z}$$

$$G^{(n)}(r_\perp) = C_1^{(n)} J_0(q_\ell r_\perp) + C_2^{(n)} N_0(q_\ell r_\perp)$$

$$F^{(n)}(r_\perp) = C_3^{(n)} J_0(q_t r_\perp) + C_4^{(n)} N_0(q_t r_\perp)$$

$$q_\ell^2 = (\omega/c_\ell)^2 - q_z^2$$

$$q_t^2 = (\omega/c_t)^2 - q_z^2$$

Bulk-like phonons:

$$\omega_{\mathbf{q}} = c_\ell q$$

$$\mathbf{u}_{\mathbf{q}} = \sqrt{\frac{\hbar}{2c_\ell \rho V}} \frac{\mathbf{q}}{q^{3/2}} e^{-i\mathbf{q}\cdot\mathbf{r}}$$

Evolution of Phonon Transport in Nanowires with "Acoustically Hard" Barriers

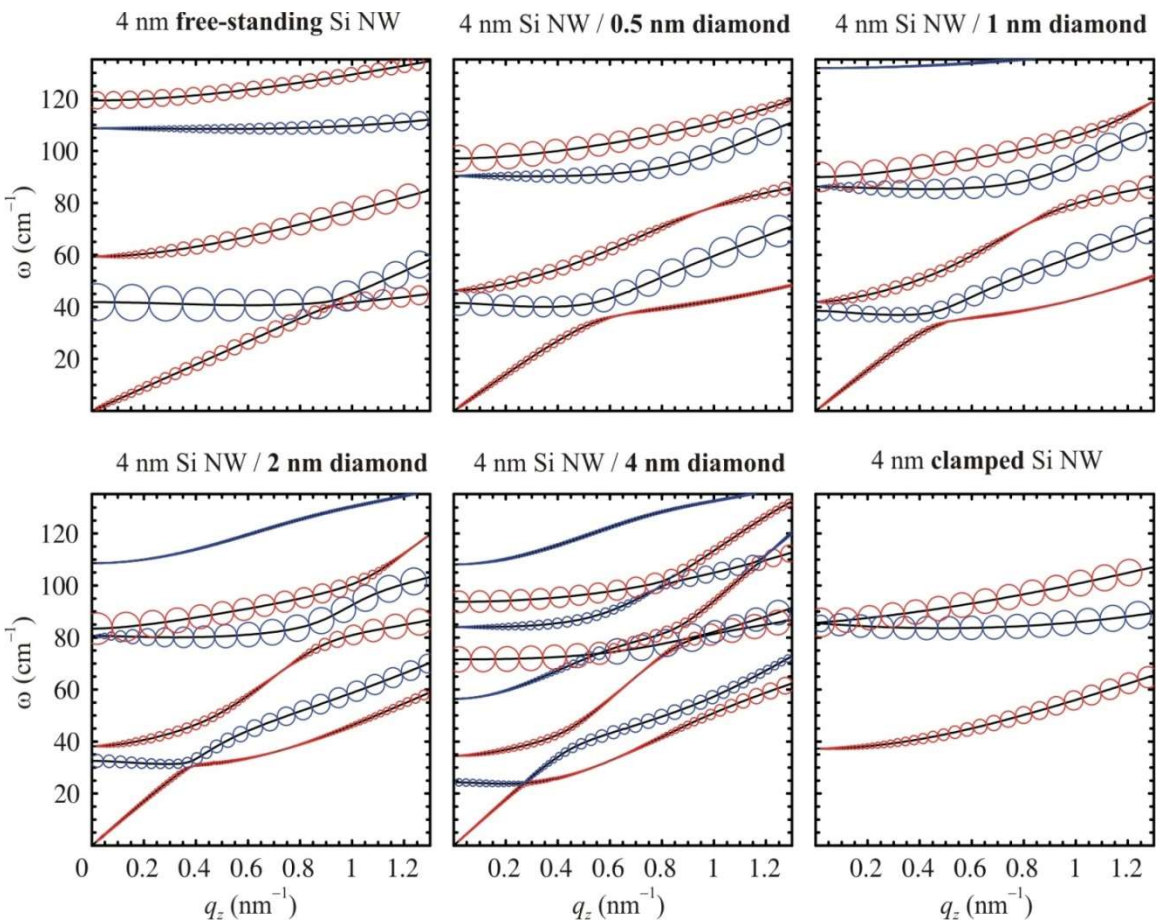

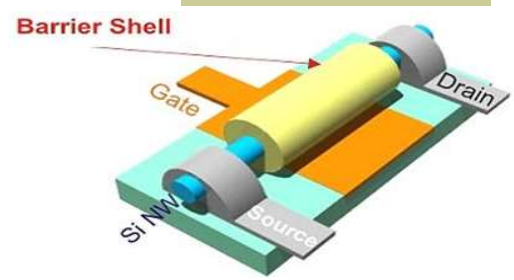

The size of the circles is proportional to the average divergence of displacement vector

Contribution of higher energy modes is negligible compared to the shown modes

"True" acoustic mode changes velocity from that in Si to the diamond

Contribution of the "true" acoustic mode to scattering decreases with increasing coating thickness

V.A. Fonoberov and A.A. Balandin, "*Nano Letters*, **6**, 2442 (2006).

Phonon Engineering of Electron Mobility in Silicon Nanowires

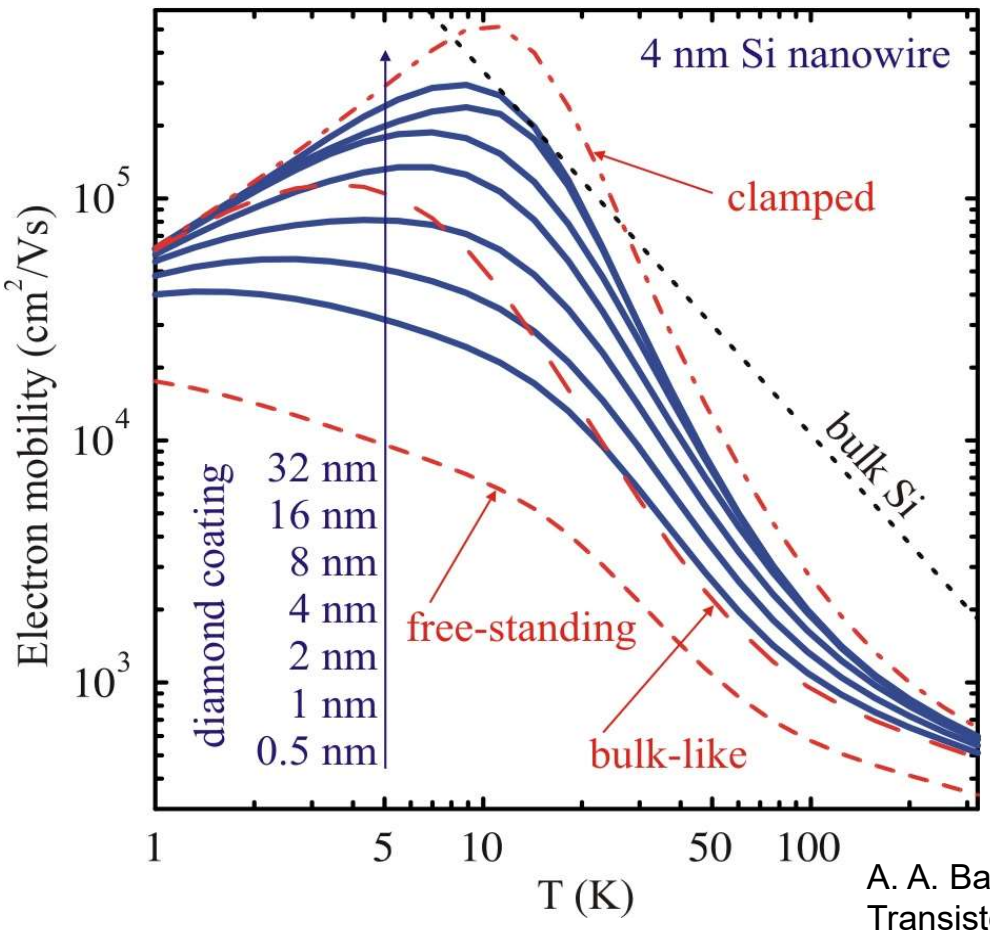

→At low T the mobility is limited by impurities and is proportional to $T^{1/2}$, while at high T it is limited by phonons and is proportional to $T^{-1/2}$

→ Electron mobility for diamond coated Si nanowire is between the limits corresponding to free-standing and clamped nanowire

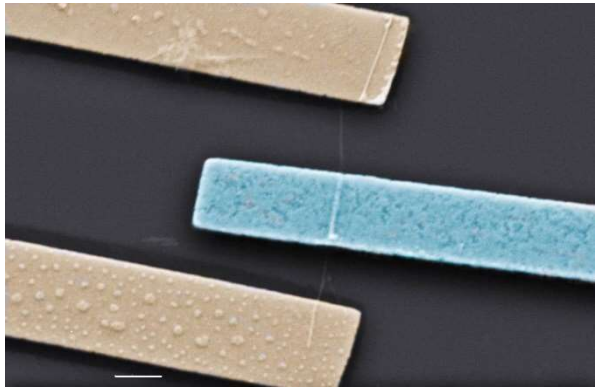

A. A. Balandin and V. A. Fonoberov, "Nanometer-Scale Transistor Architecture Providing Enhanced Carrier Mobility," U.S. Patent 8,097,922

Experimental Evidence of Phonon Confinement Effects in GaN Nanowires

Brillouin-light-scattering measurements and finite-element modeling of vibrational spectra in mono-crystalline GaN nanowires

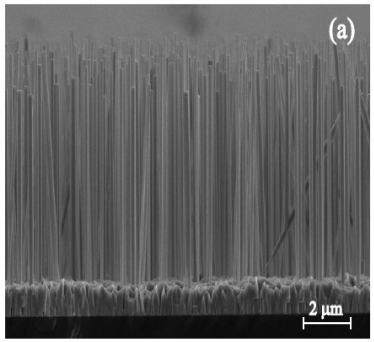

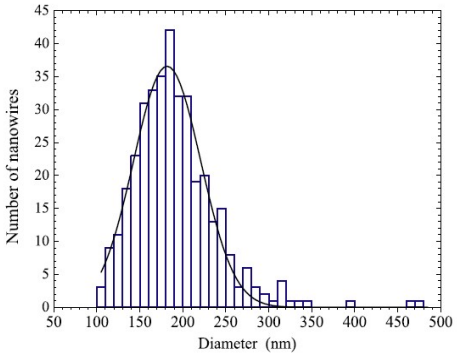

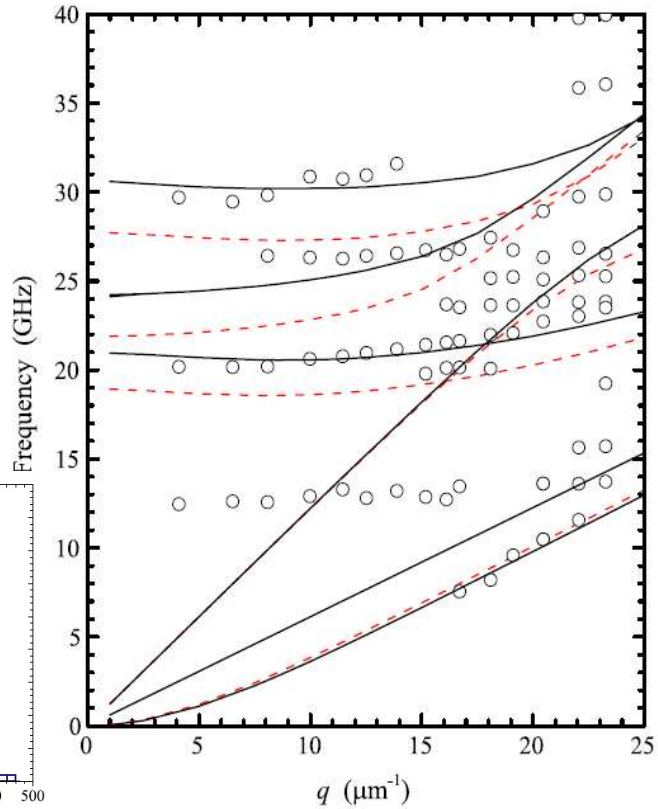

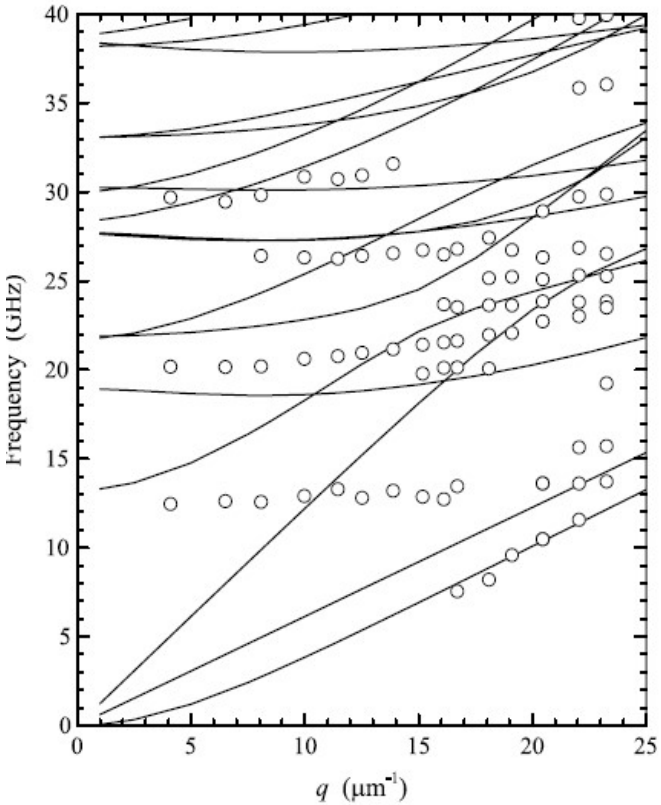

W.L. Johnson *et al.*, *Nanotechnology*, **23**, 495709 (2012).

Experimental Evidence of Phonon Confinement Effects in Nanostructures

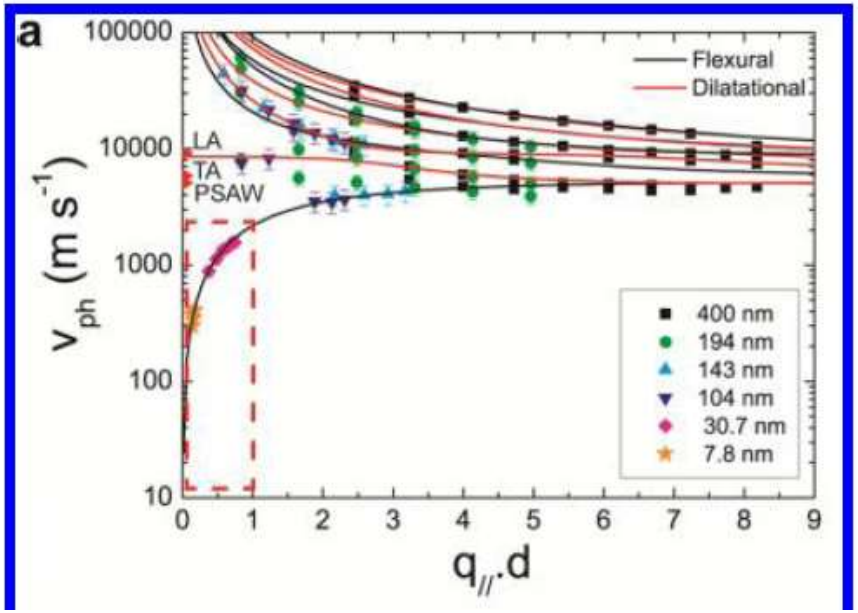

"We report the changes in dispersion relations of hypersonic acoustic phonons in free-standing silicon membranes as thin as ~8 nm. We observe a reduction of the phase and group velocities of the fundamental flexural mode by more than 1 order of magnitude compared to bulk values."

J. Cuffer et al., *Nano Lett.*, **12**, 3569 (2012).

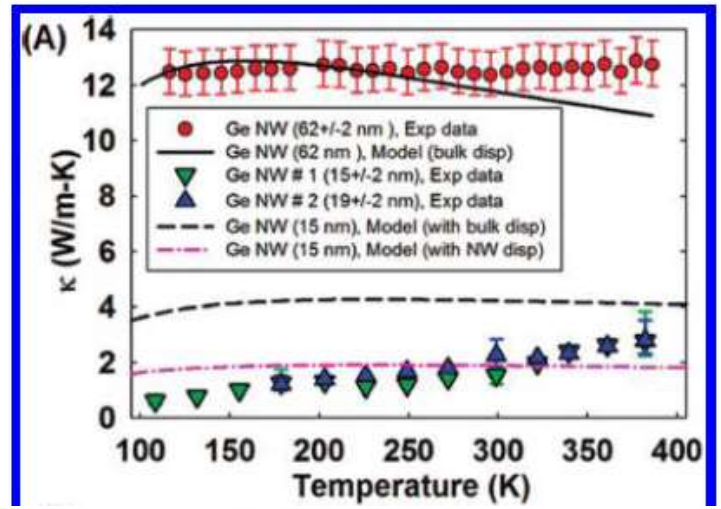

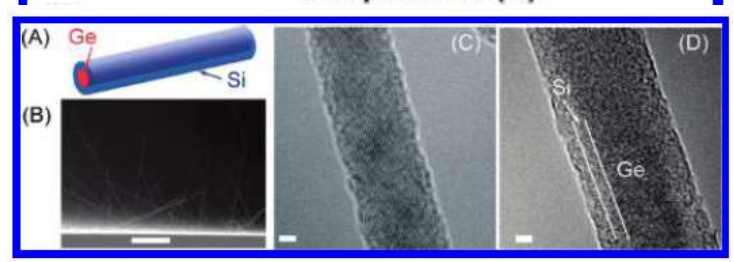

"Thermal conductivities of the sub-20 nm diameter NWs are further suppressed by the phonon confinement effect beyond the diffusive boundary scattering limit."

M.C. Wingert et al., *Nano Lett.*, **11,** 5507 (2011).

Part II: Phonons in Graphene

←*IEEE Spectrum* illustration of the discovery of unique thermal properties of graphene at UC Riverside (IEEE Spectrum, October, 2009)

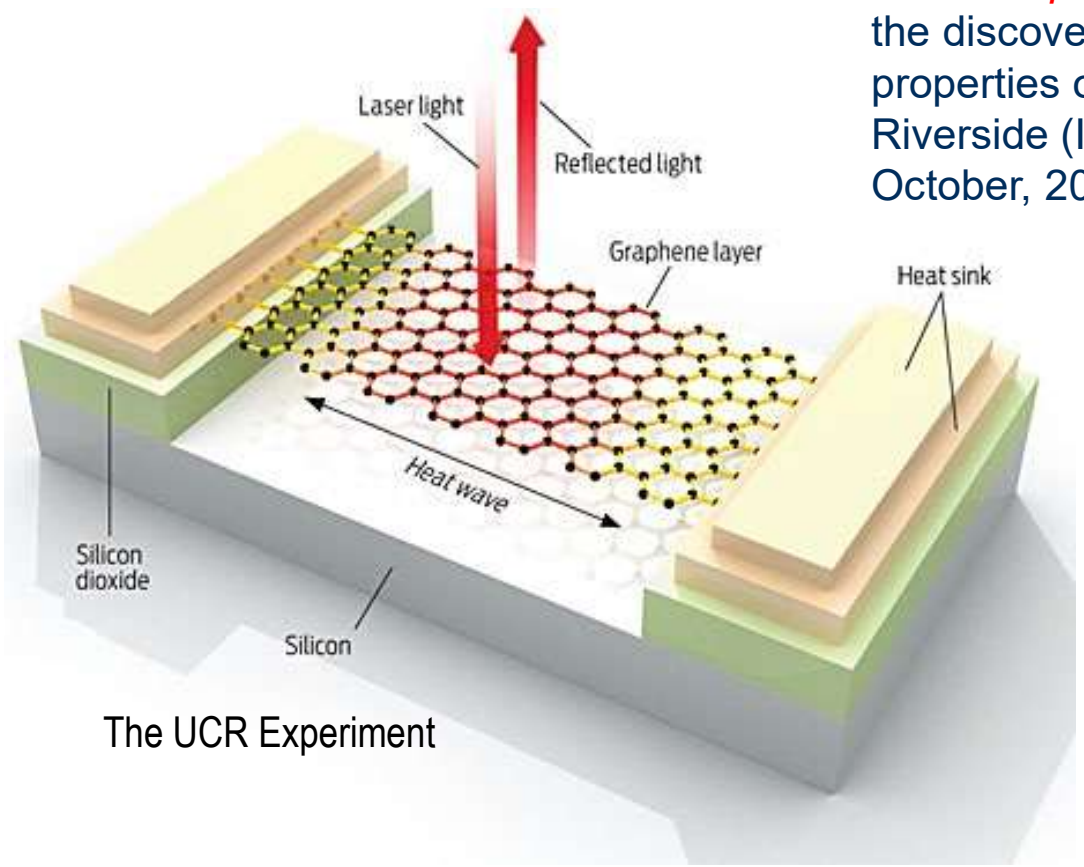

The UCR Experiment

Optical Phonons in Graphene: Raman Spectroscopy

Visualization on Si/SiO_2 substrates

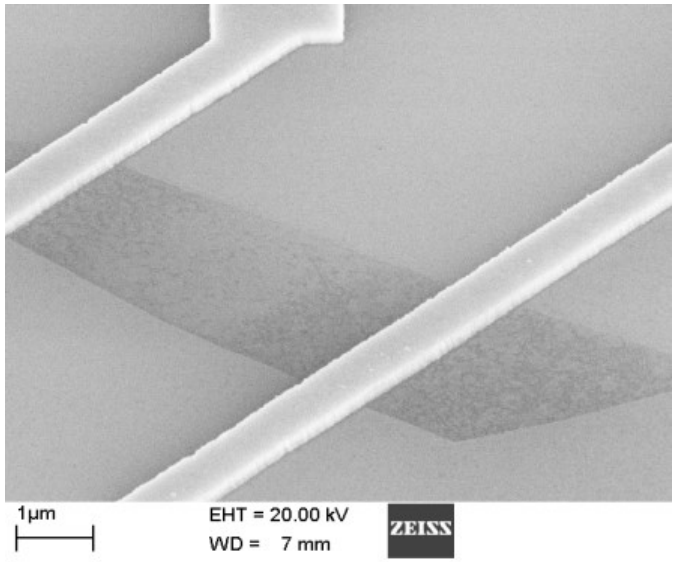

Other techniques:

→ low-temperature transport study

→ cross-sectional TEM

→ few other costly methods

***D band*: A_{1g} (~1350 cm^{-1}); *G peak:* E_{2g}; *2D* band**

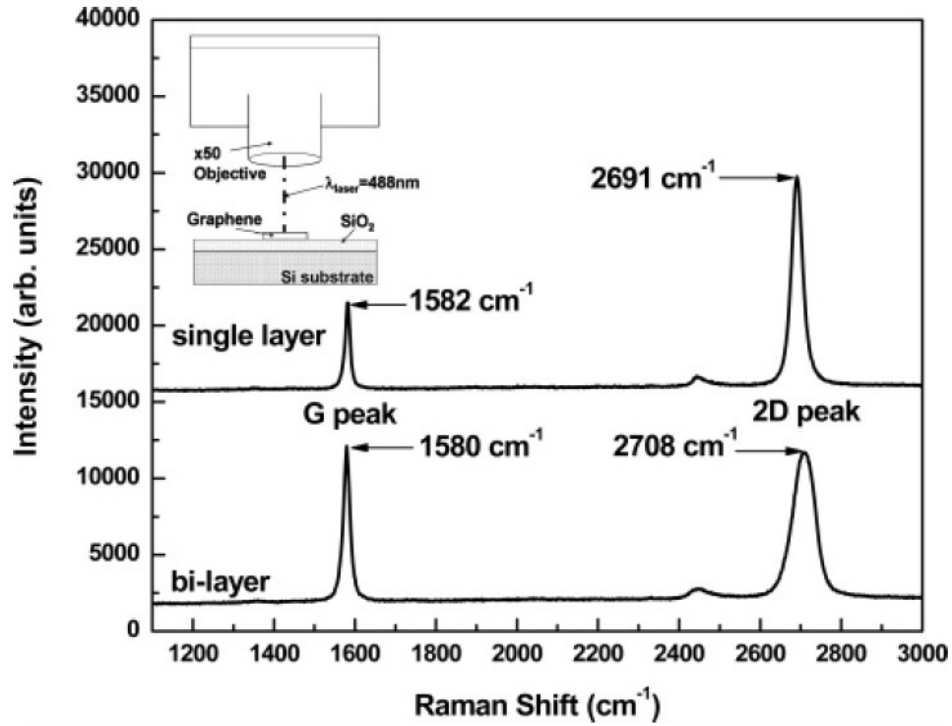

A.C. Ferrari et al., *Phys. Rev. Lett.* **97**, 187401 (2006).

I. Calizo, et al., *Nano Lett.*, **7**, 2645 (2007).

Temperature Effects on Raman Spectrum – Converting Spectrometer into "Thermometer"

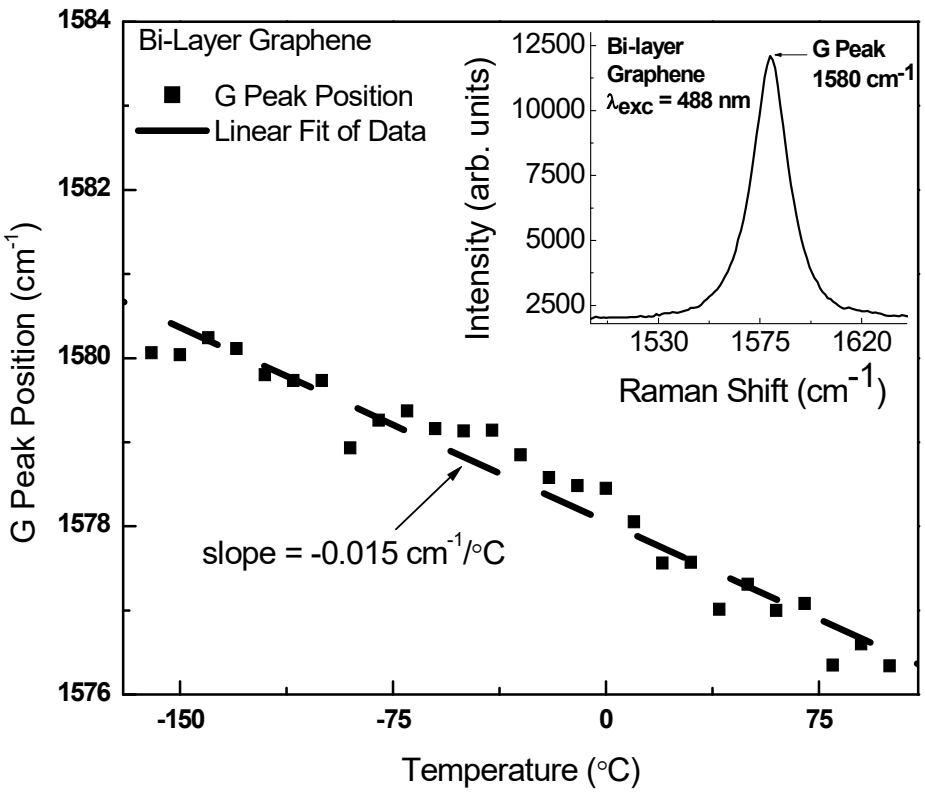

Optothermal technique for measuring thermal conductivity of graphene

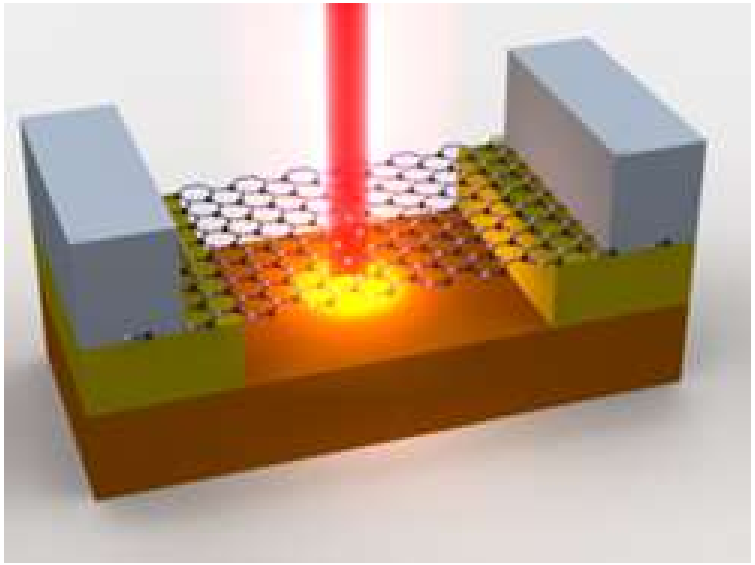

Temperature is controlled externally; very low excitation power on the sample surface is used (< 0.5 – 1 mW).

Phonon frequency downshift with T is unusual when the bond-bond distances shorten with T since normally lattice contraction leads to the upward shift of the frequencies.

Raman Optothermal Measurement Procedure for Graphene

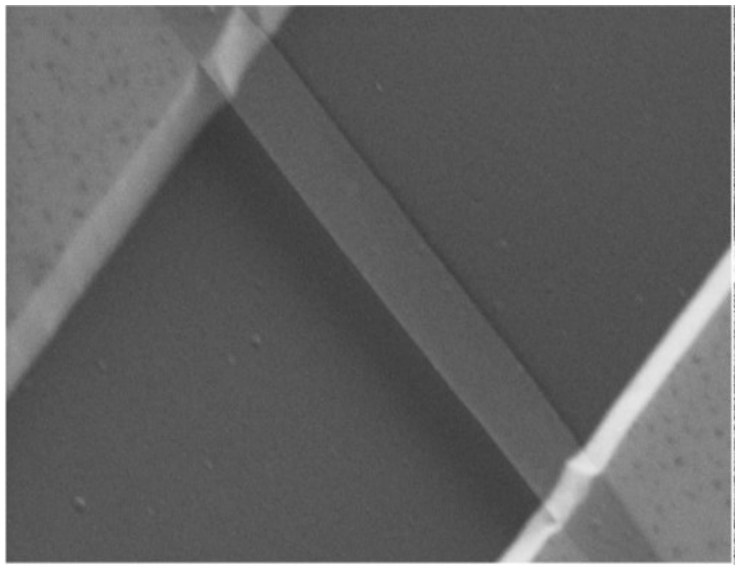

Bilayer graphene ribbon bridging 3-μm trench in Si/SiO_2 wafer

$$K = (L / 2 a_G W) \chi_G (\Delta \omega / \Delta P_G)^{-1}.$$

Connect ΔP_D ← → ΔP_G through calibration

→ Laser acts as a heater: ΔP_G

→ Raman "thermometer": $\Delta T_G = \Delta\omega / \chi_G$

→ Thermal conductivity: $K = (L/2a_G W)(\Delta P_G / \Delta T_G)$

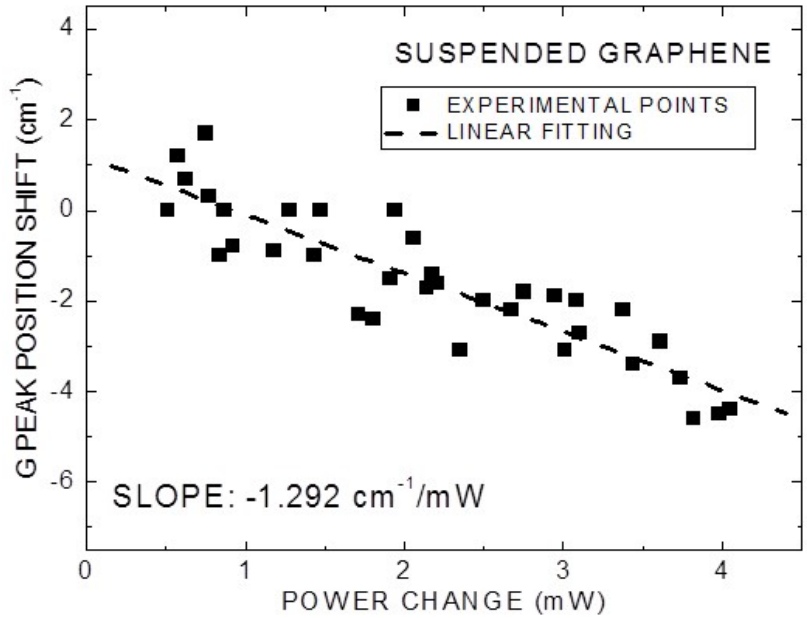

A.A. Balandin, et al., *Nano Letters*, **8**, 902 (2008).

Evolution of the Intrinsic Thermal Conductivity in Low-Dimensional Systems

Experiment and Umklapp Scattering Theory

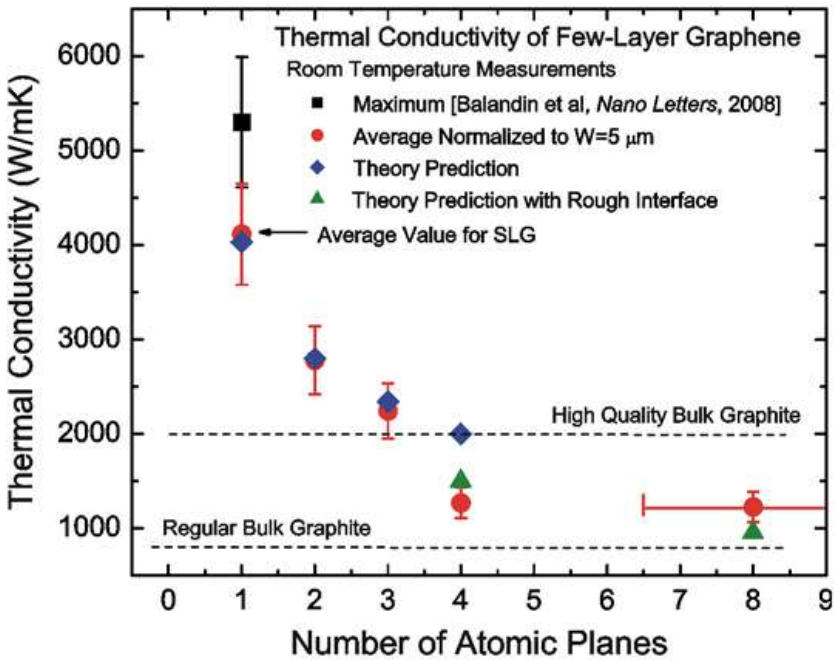

S. Ghosh, W. Bao, D.L. Nika, S. Subrina, E.P. Pokatilov, C.N. Lau and A.A. Balandin, "Dimensional crossover of thermal transport in few-layer graphene," *Nature Materials*, **9**, 555 (2010).

Nonequilibrium Molecular Dynamics Study

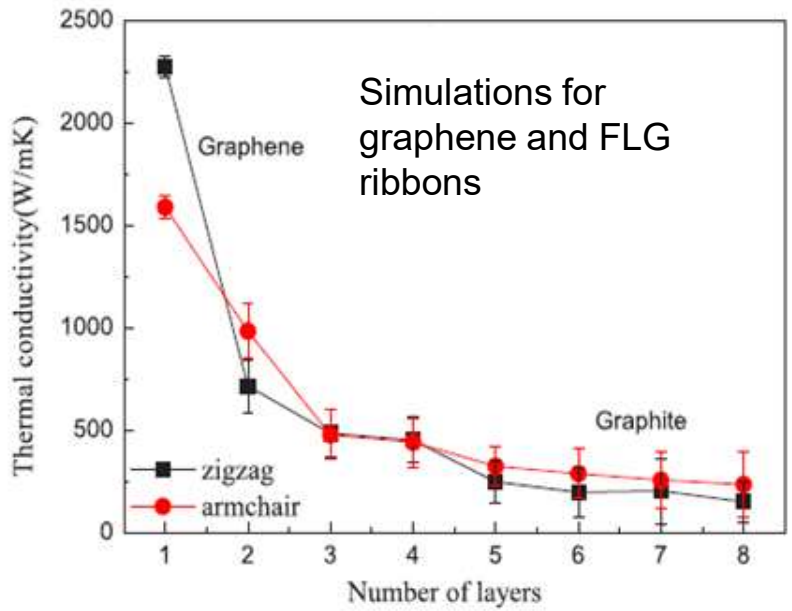

W.-R. Zhong et al., *Appl. Phys. Lett.*, **98**, 113107 (2011).

Consistent with the prediction:

S. Berber,Y.-K. Kwon, and D. Tomanek, *Phys. Rev. Lett.*, **84**, 4613 (2000).

Phonons in Isotopically Engineered Graphene

Cooperation with Ruoff Group

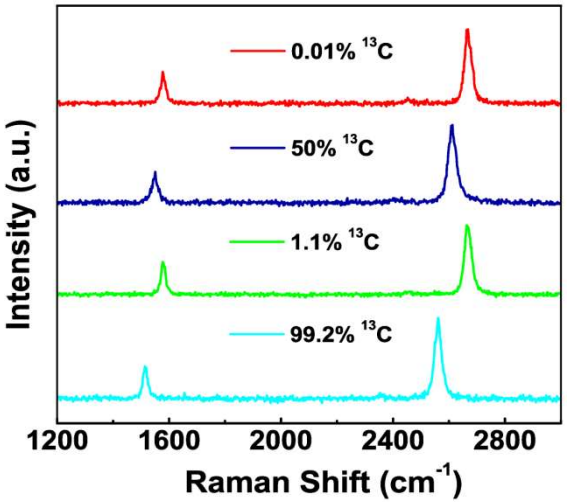

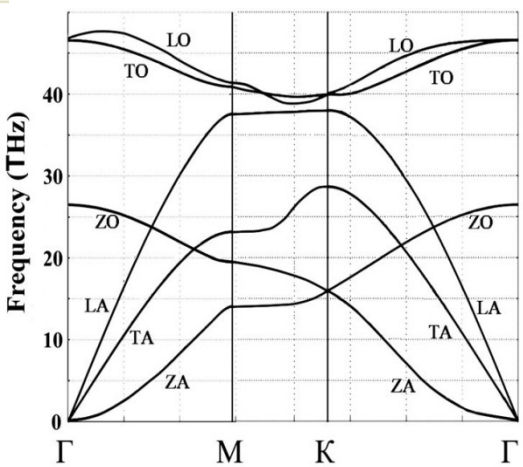

^{13}C and ^{12}C difference: ~ 64 cm^{-1}

$$\omega \propto M^{-1/2}$$

The thermal conductivity, K, of isotopically pure ^{12}C (0.01% ^{13}C) graphene was higher than 4000 W/mK at T~320 K and more than a factor of two higher than in 50%-50% ^{12}C and ^{13}C graphene.

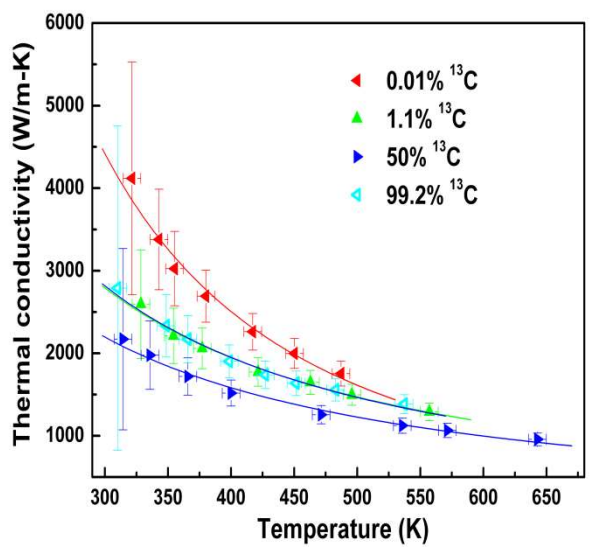

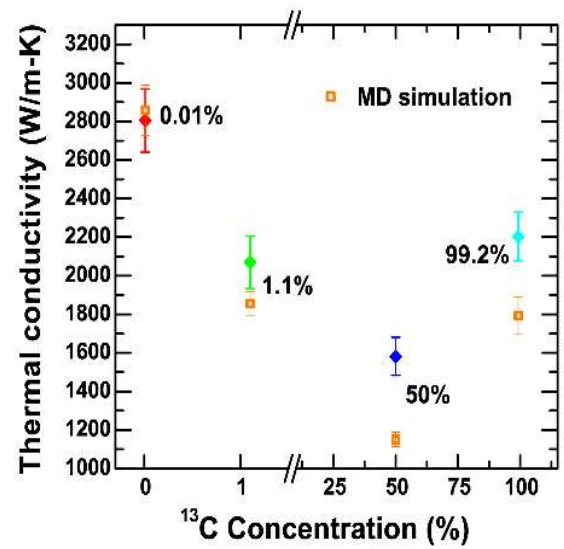

S. Chen, Q. Wu, C. Mishra, J. Kang, H. Zhang, K. Cho, W. Cai, A.A. Balandin and R.S. Ruoff, "Thermal conductivity of isotopically modified graphene," *Nature Materials*, 11, 203 (2012).

Klemens Model of Heat Conduction: Bulk Graphite vs. Graphene

Phonon Thermal Conductivity:

$$K_p = \Sigma_j \int C_j(\omega)\upsilon_j^2(\omega)\tau_j(\omega)d\omega$$

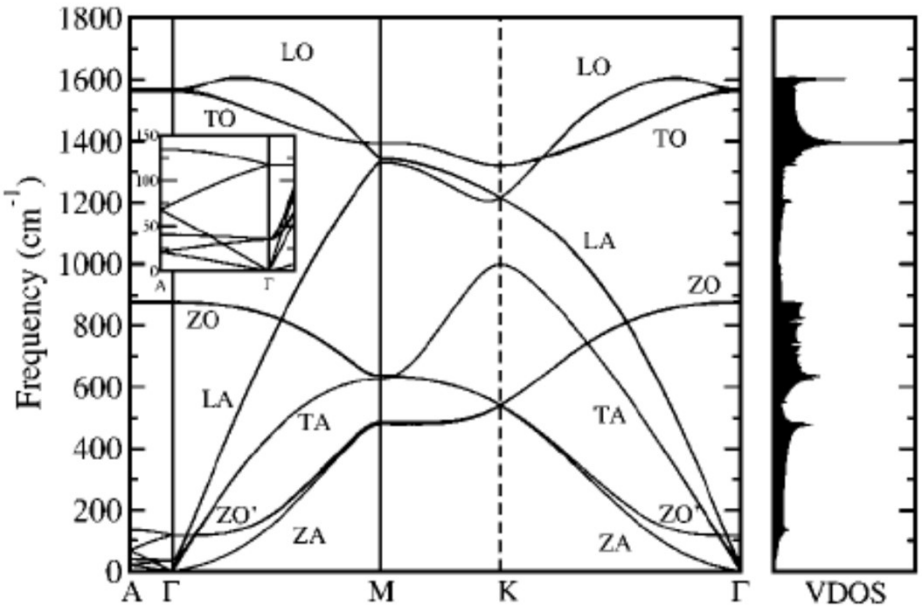

P.G. Klemens, *J. Wide Bandgap Materials*, **7**, 332 (2000).

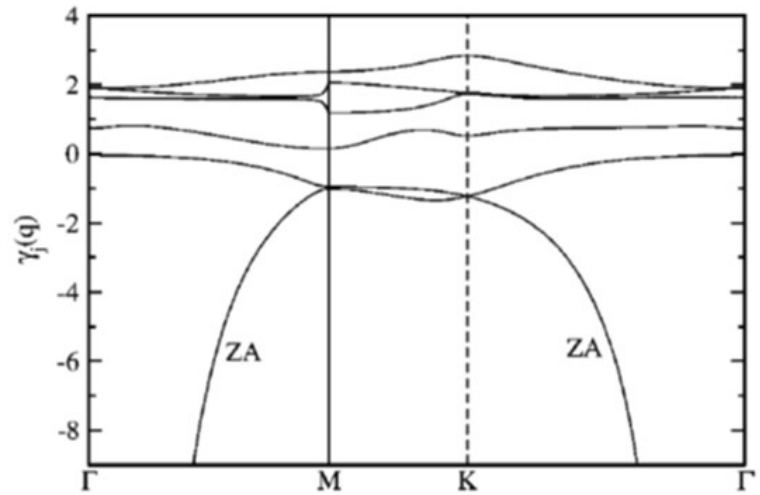

N. Mounet et al, *Phys. Rev. B* **71**, 205214 (2005).

Umklapp life-time, which defines MFP:

$$\tau_{U,s} = \frac{1}{\gamma_s^2}\frac{M\upsilon_s^2}{k_B T}\frac{\omega_{s,\max}}{\omega^2} \qquad \gamma_{\lambda,k} = -\frac{\partial \ln(\omega_{\lambda,k})}{\partial \ln V}$$

2-D: $C(\omega) \sim \omega \rightarrow K \sim T^{-1}\omega^{-1}$

3-D: $C(\omega) \sim \omega^2$

The Role of the Long-Wavelength Phonons in Heat Transport in Graphene

Thermal conductivity in graphene:

$$K \propto \frac{1}{\omega_m}\int_{\omega_C}^{\omega_m}\frac{d\omega}{\omega} \propto \frac{1}{\omega_m}\ln\left(\frac{\omega_m}{\omega_C}\right).$$

Graphene:

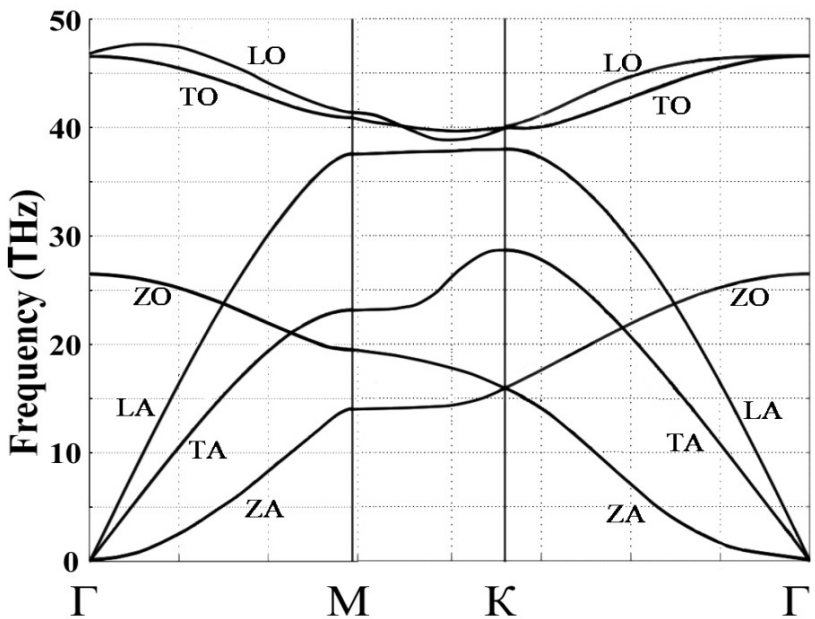

MFP = L – physical size of the system

→ Limitation on MFL: $L = \tau v_s$

$$\tau_{U,s} = \frac{1}{\gamma_s^2}\frac{M\upsilon_s^2}{k_B T}\frac{\omega_{s,\max}}{\omega^2}$$

→ Limiting low-bound frequency:

$$\omega_{s,\min} = \frac{\upsilon_s}{\gamma_s}\sqrt{\frac{M\upsilon_s}{k_B T}\frac{\omega_{s,\max}}{L}}$$

$$K = (2\pi\gamma^2)^{-1}\rho(\upsilon^4 / f_m T)\ln(f_m / f_B),$$

$$f_B = \left(M\upsilon^3 f_m / 4\pi\gamma^2 k_B T L\right)^{1/2}$$

Alexander A. Balandin, University of California – Riverside

Divergence of the Lattice Thermal Conductivity in 2-D Crystal Lattices

K ~ log(N) in 2D

K ~ N^{α} in 1D, $\alpha \neq 1$

N – system size

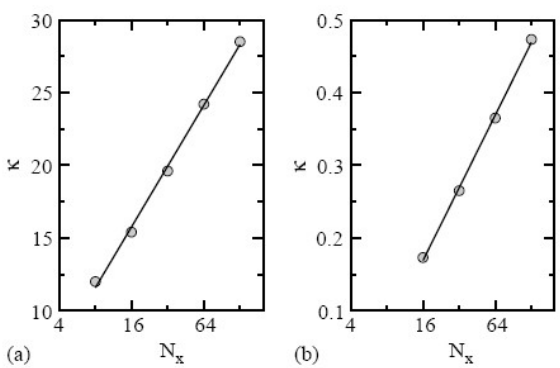

Thermal conductivity in 2D lattice vs. N_x. Data is after S. Lepri et al. (Ref. [8]).

→ *Consensus*: The intrinsic thermal conductivity of 2-D or 1-D anharmonic crystals is anomalous.

[1] K. Saito, et al., *Phys. Rev. Lett.* 104, 040601 (2010).
[2] A. Dhar. *Advances in Physics* 57, 457 (2008).
[3] G. Basile et al. *Eur. Phys. J.* 151, 85 – 93 (2007).
[4] L. Yang et al. *Phys. Rev. E* 74, 062101 (2006).
[5] L. Delfini et al. *Phys, Rev. E* 73, 060201R (2006).
[6] S. Lepri et al. *Chaos* 15, 015118 (2005).
[7] J. Wang, B. Li. *Phys. Rev. Lett*. 92, 074302 (2004).
[8] S. Lepri et al. *Phys. Rep.* 377, 1 (2003).
[9] R. Livi and S. Lepri. *Nature* 421, 327 (2003).
[10] O. Narayan et al., *Phys. Rev. Lett*., 89, 20601 (2002).
[11] A. Dhar. *Phys. Rev. Lett*. 86, 5882 (2001).
[12] A. Lepri and R. Livi, *J. Stat. Phys*. 100, 1147 (2000).
[13] T. Pozen et al., Phys. Rev. Lett., 84, 2857 (2000).
[14] S. Lepri et. al. *Europhys. Lett*. 43, 271 (1998).

Uniqueness of Heat Conduction in Graphene

Breakdown of Fourier's Law vs. Size-Dependent Intrinsic Thermal Conductivity

The phonon transport in graphene is 2D all the way down to zero frequency

Low-bound cut-off frequency is defined by the condition that the phonon MFP can not exceed the physical size of the graphene flake:

$$\omega_{s,\min} = \frac{\upsilon_s}{\gamma_s}\sqrt{\frac{M\upsilon_s}{k_B T}\frac{\omega_{s,\max}}{L}}$$

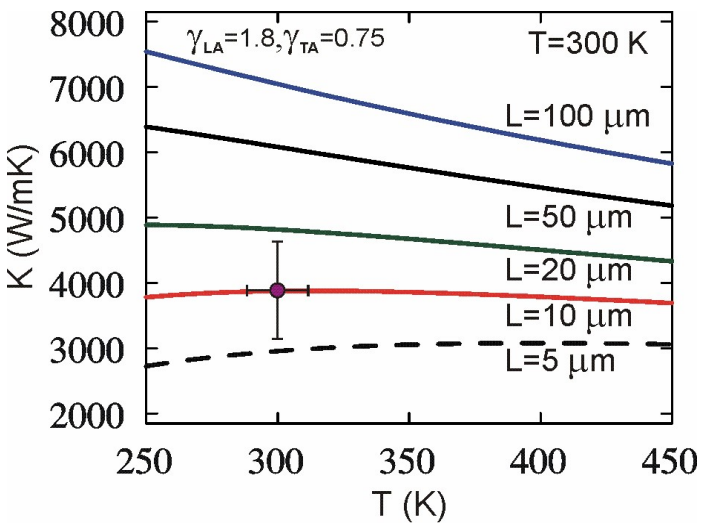

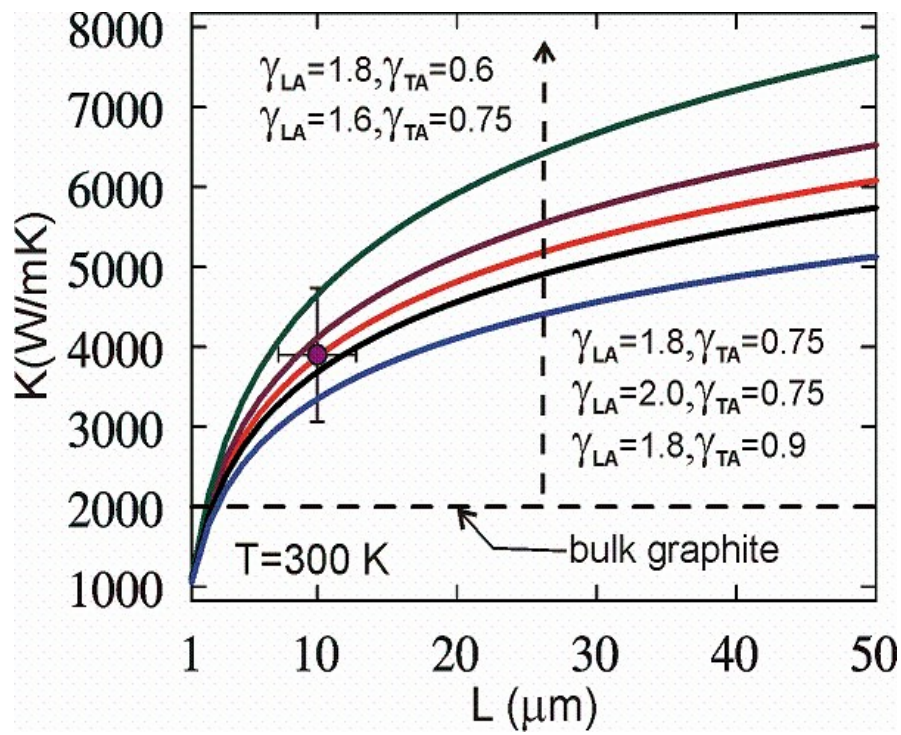

D.L. Nika, S. Ghosh, E.P. Pokatilov, A.A. Balandin, *Appl. Phys. Lett.*, **94**, 203103 (2009).

Engineering Phonons by Twisting Atomic Planes

Phonons in Twisted Bilayer Graphene

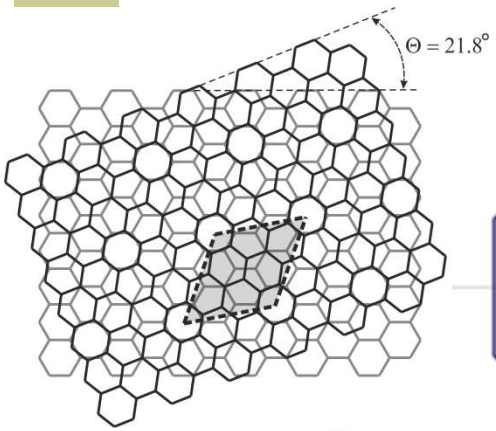

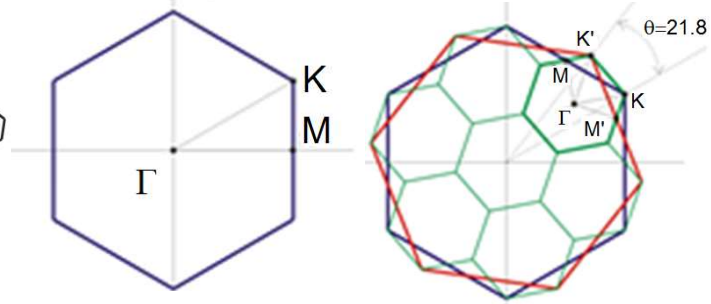

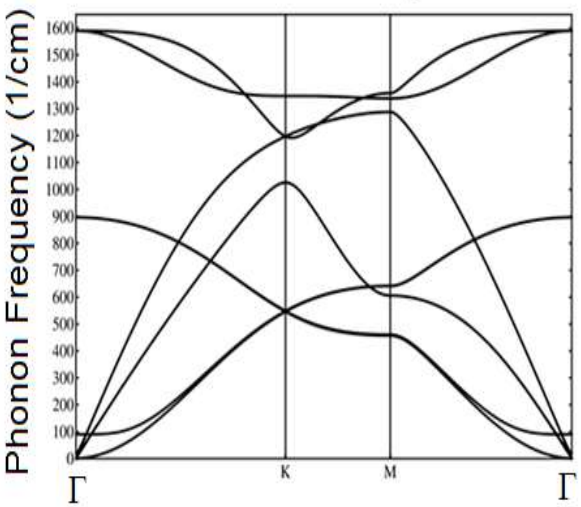

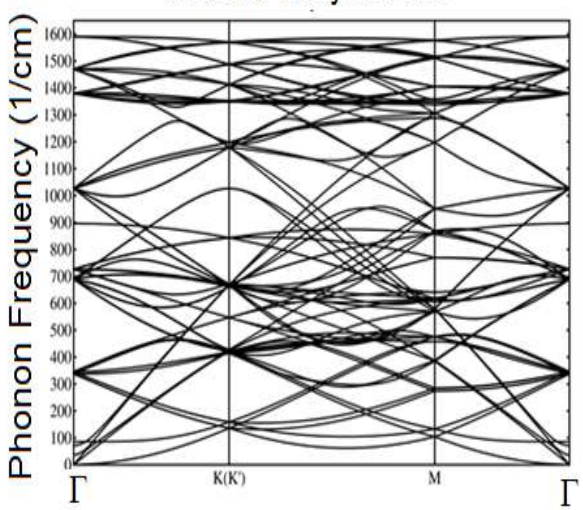

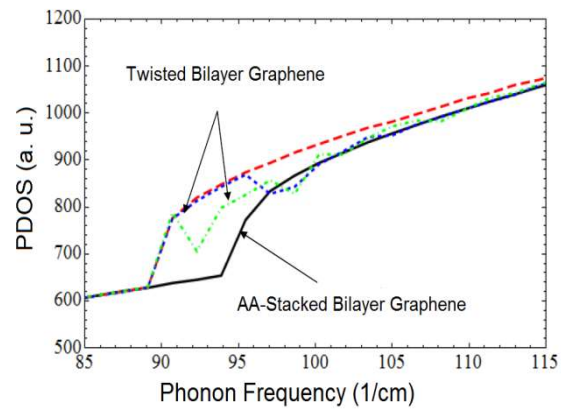

→ Born-von Karman model for description of the carbon-carbon intra-layer interactions

→ Lennard-Jones potential for the inter-layer interactions

A.I. Cocemasov, D.L. Nika and A.A. Balandin, "Phonons in twisted bilayer graphene" Phys. Rev. B, 88, 035428 (2013)],

Please see POSTER for details

Part III: Phonons in van der Waals Materials

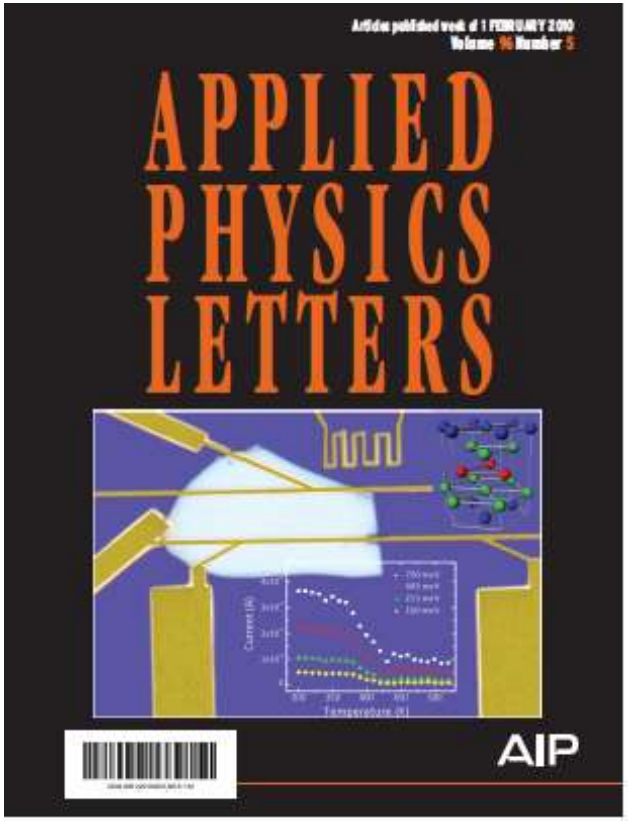

← D. Teweldebrhan, V. Goyal, M. Rahman and A.A. Balandin, "Atomically-thin crystalline films and ribbons of bismuth telluride," Applied Physics Letters, 96, 053107 (2010). - *Issue's Cover*

Van der Waals Materials: Two-Dimensional Materials Beyond Graphene

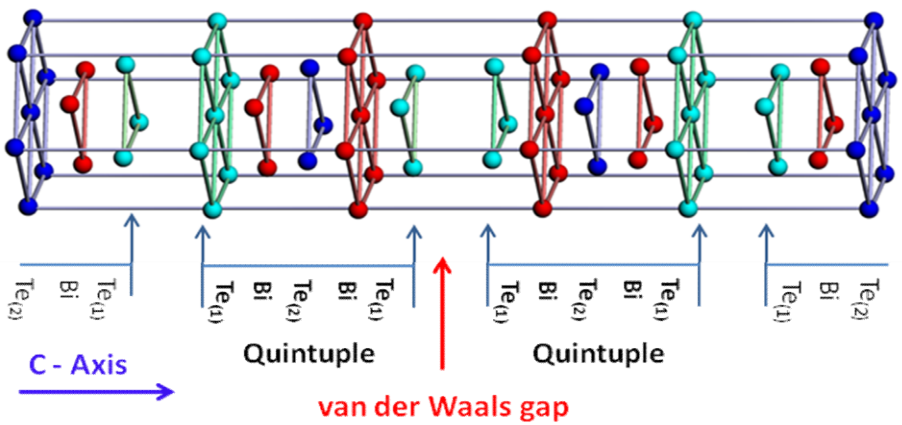

Topological Insulators

→ Benefits of Few-Quintuple Films

→ Predicted High Thermoelectric Figure of Merit

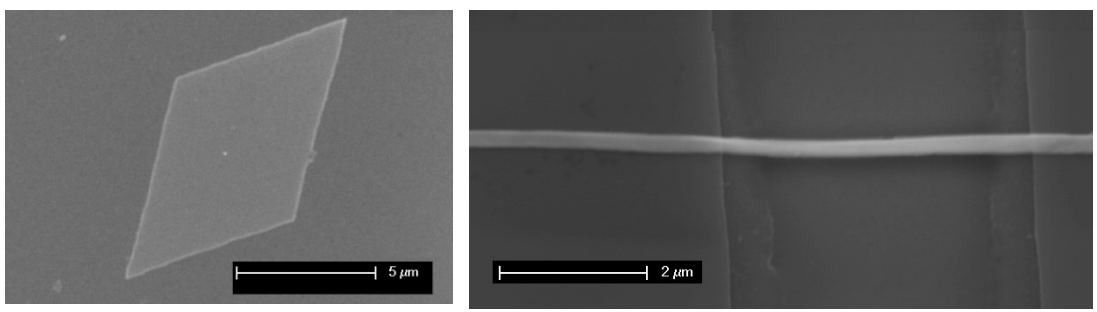

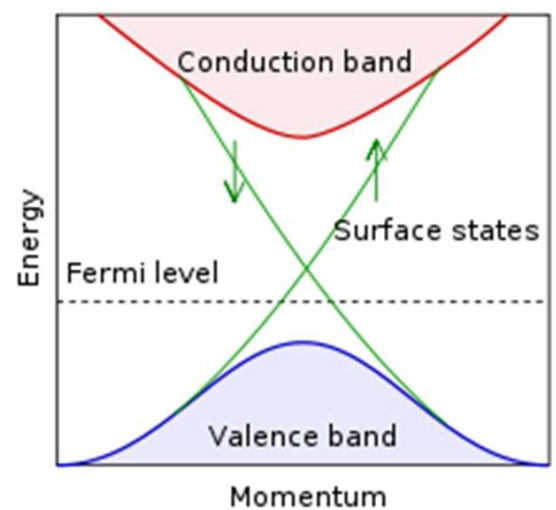

D. Teweldebrhan, V. Goyal and A.A. Balandin, "Exfoliation and characterization of bismuth telluride atomic *quintuples* and quasi-2D crystals," *Nano Letters*, 10, 1209 (2010).

Thermoelectric Motivation for Atomically Thin Films of Bi_2Te_3

The thermoelectric figure of merit: $ZT=S^2\sigma T/(K_e+K_p)$

S is the Seebeck coefficient, σ is the electrical conductivity and *K* is the thermal conductivity.

Electron Quantum Confinement

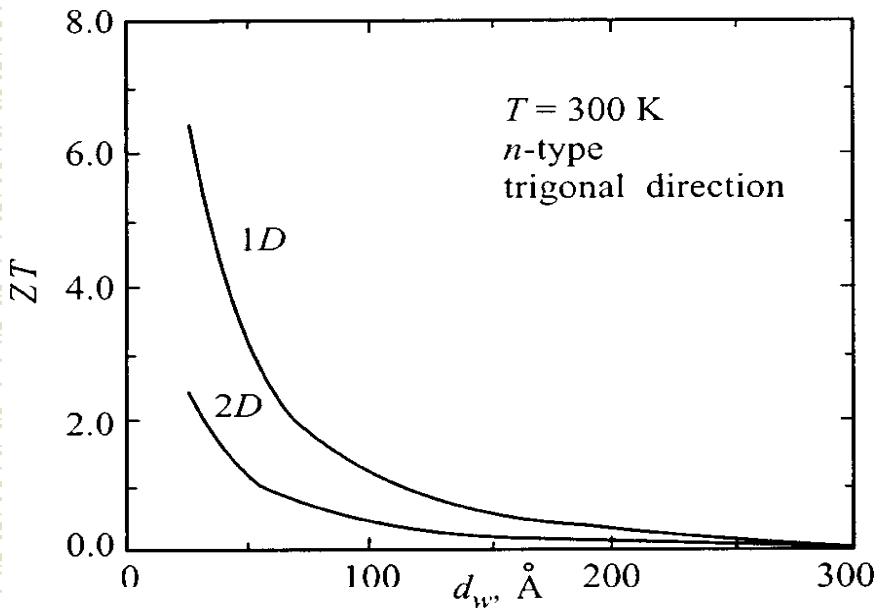

M.S. Dresselhaus, et al. *Phys. Solid State* (1999).
L.D. Hicks and M.S. Dresselhaus, *Phys. Rev. B* (1993).

Acoustic Phonon Confinement

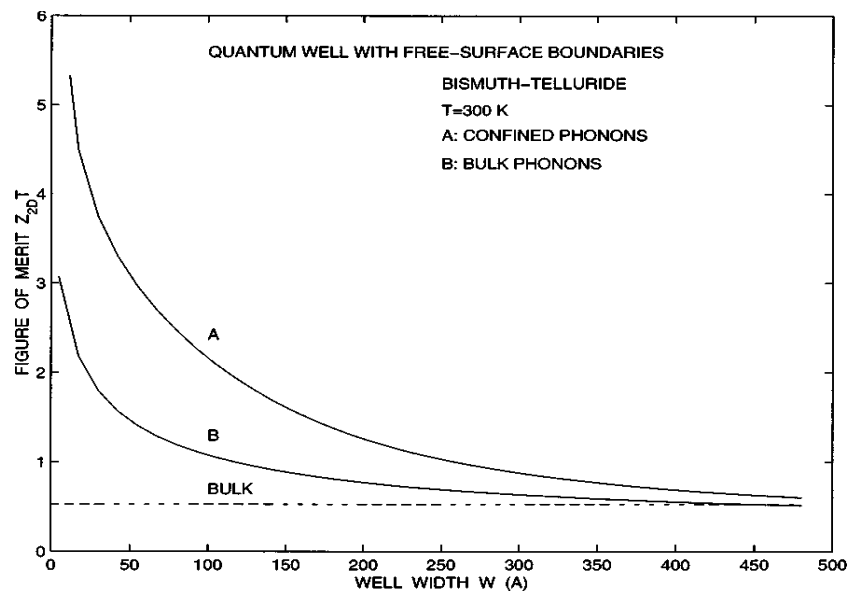

A.A. Balandin and K.L. Wang, *Phys. Rev. B* (1998).
A.A. Balandin and K.L. Wang, *J. Appl. Phys*. (1998).

Low potential barrier in Bi_2Te_3/Bi_2Se_3; Bi_2Te_3/Sb_2Te_3

Raman Spectroscopy of the Atomically Thin Films of Bi-Te Topological Insulators

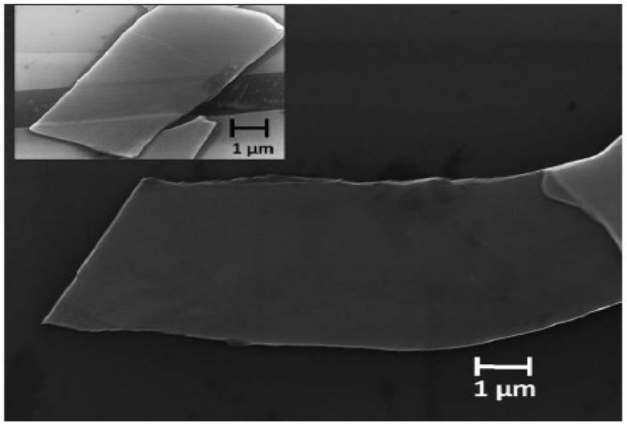

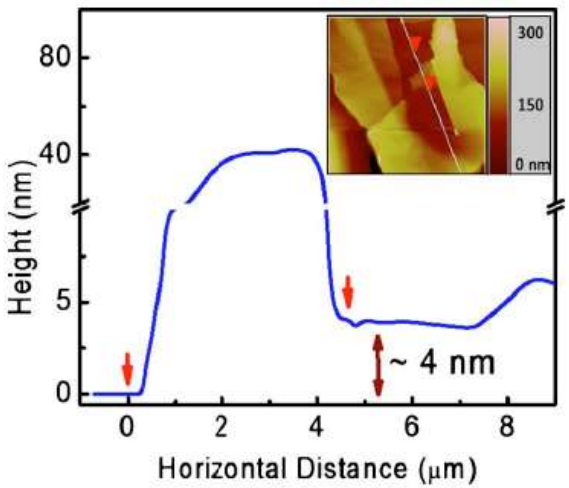

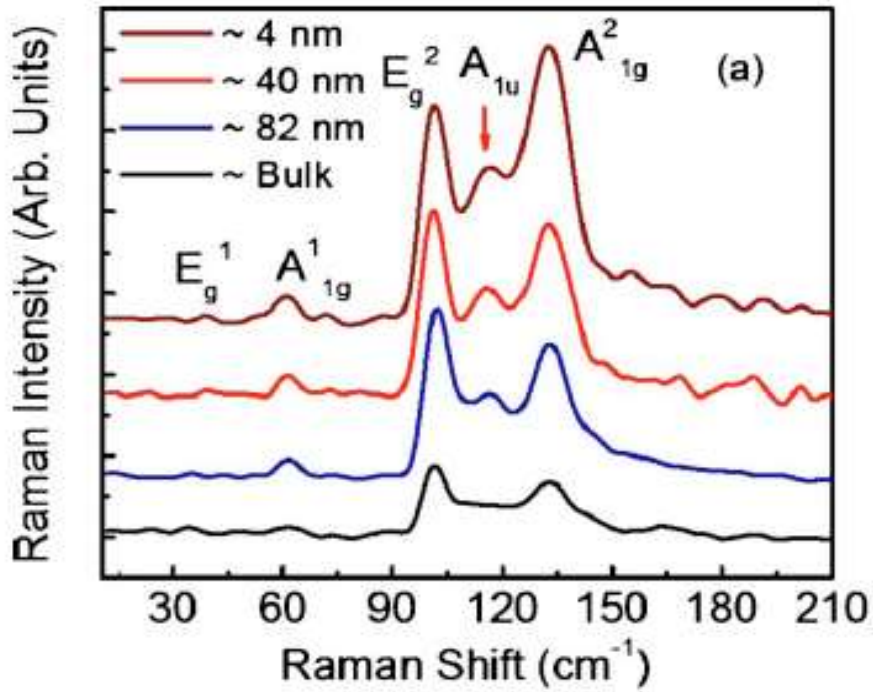

K.M.F. Shahil, M.Z. Hossain, D. Teweldebrhan and A.A. Balandin, "Crystal symmetry breaking in few-quintuple Bi_2Te_3 films: Applications in nanometrology of topological insulators," *Appl. Phys. Lett.*, **96**, 153103 (2010).

Room-Temperature Electrical Characterization Bi-Te Atomic Films

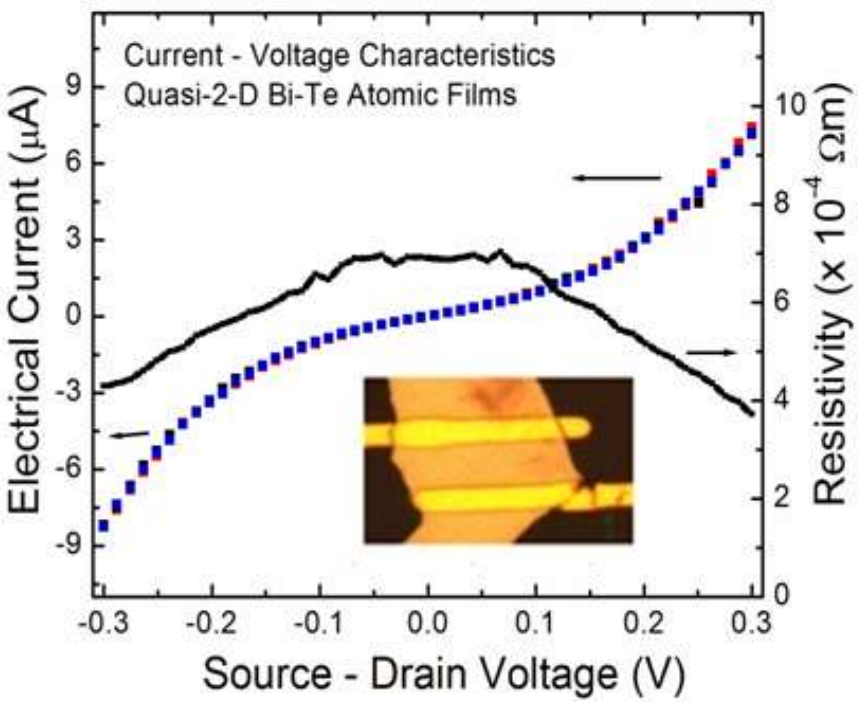

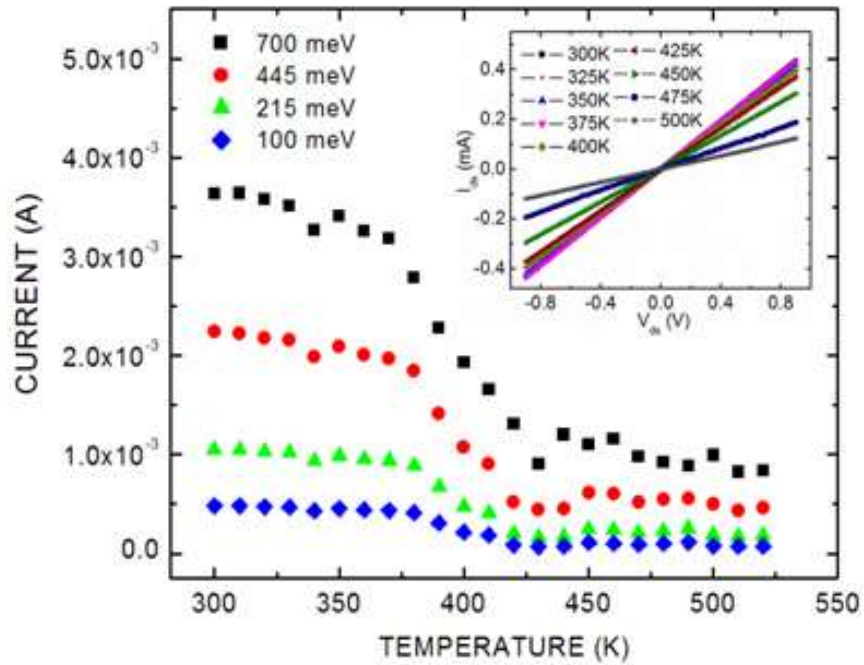

→Weak gating at RT

→ Resistivity is ~10^{-4} Ωm

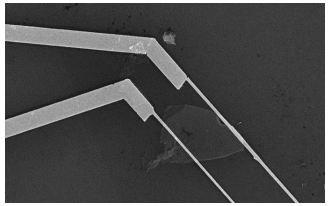

D. Teweldebrhan, V. Goyal, M. Rahman and A.A. Balandin, "Atomically-thin crystalline films and ribbons of bismuth telluride," *Appl. Phys. Lett.*, **96**, 053107 (2010).

Thermoelectric Energy Conversion with Stacks of Bi_2Te_3 Exfoliated Films

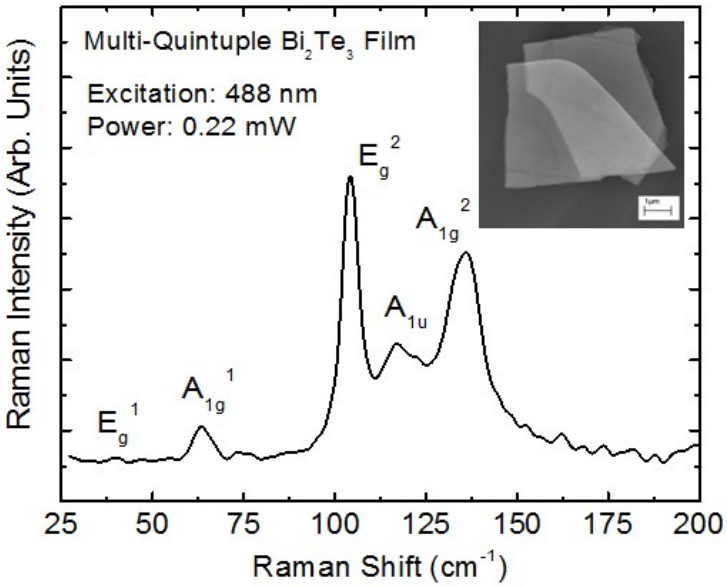

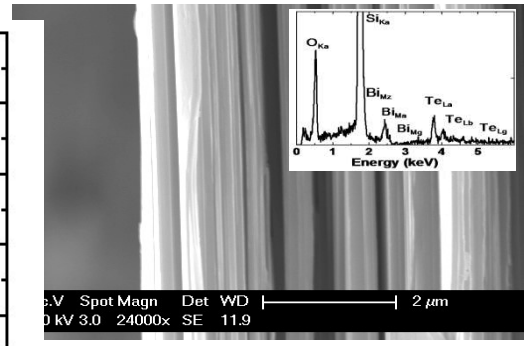

V. Goyal, D. Teweldebrhan and A.A. Balandin, "Mechanically exfoliated stacks of thin films of Bi_2Te_3 topological insulator films", Appl. Phys. Lett. (2010).

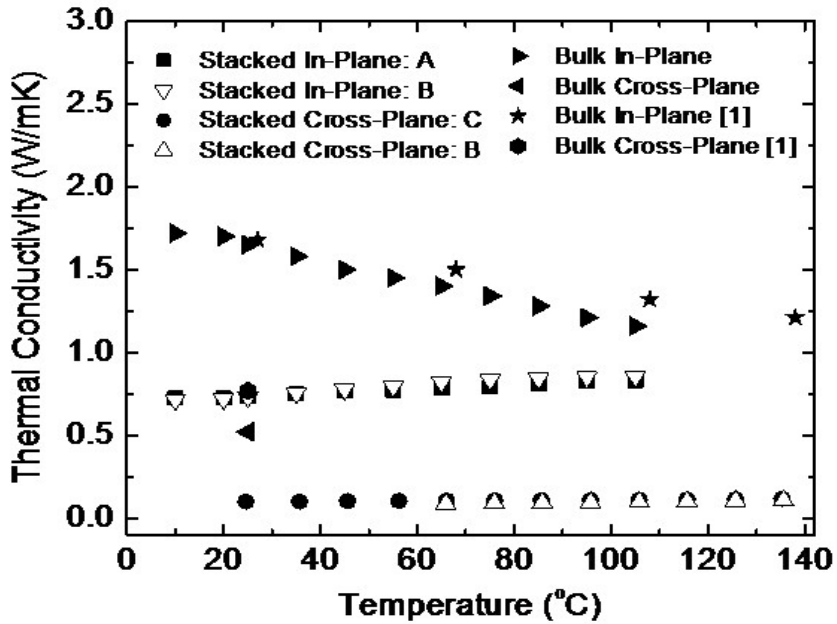

ZT increase by ~140 – 250% at room temperature

The enhancement is expected to be larger at low T

Charge Density Waves: Macroscopic Quantum State

Normal state $T > T_c$

Electron Density $\rho_e = const$

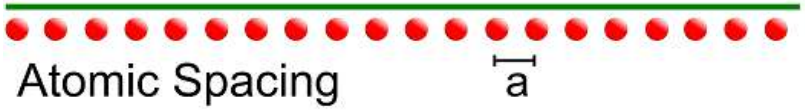

Atomic Spacing

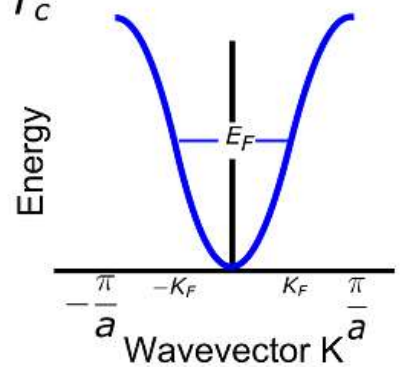

Peierls state $T < T_c$

Electron Density $\rho_e = \rho_0 + \rho_1 cos(qx + \lambda_c)$

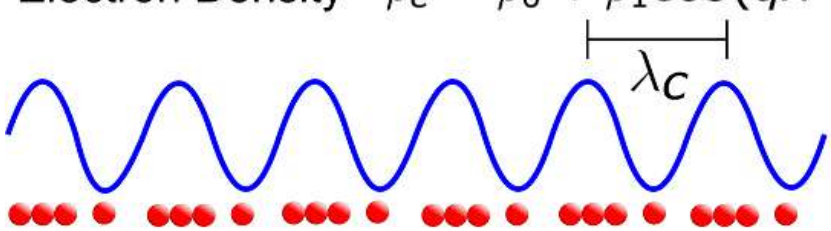

Atomic Spacing

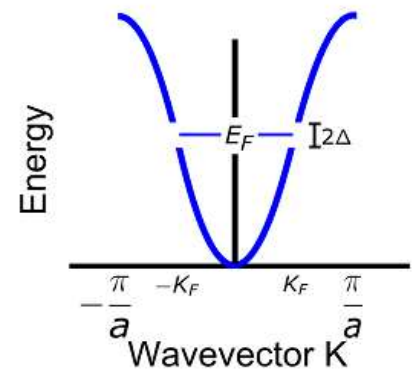

- → CDW is a cooperative state of the ionic lattice and electron gas
- → 1D and 2D metal-chalcogenides: $NbSe_2$, $NbSe_3$, TaS_2, $TiSe_2$
- → CDW can move in electric field
- → Progress in 1970 – 1980

Phonon Spectrum Evolution with the $TiSe_2$ Film Thickness

$TiSe_2$

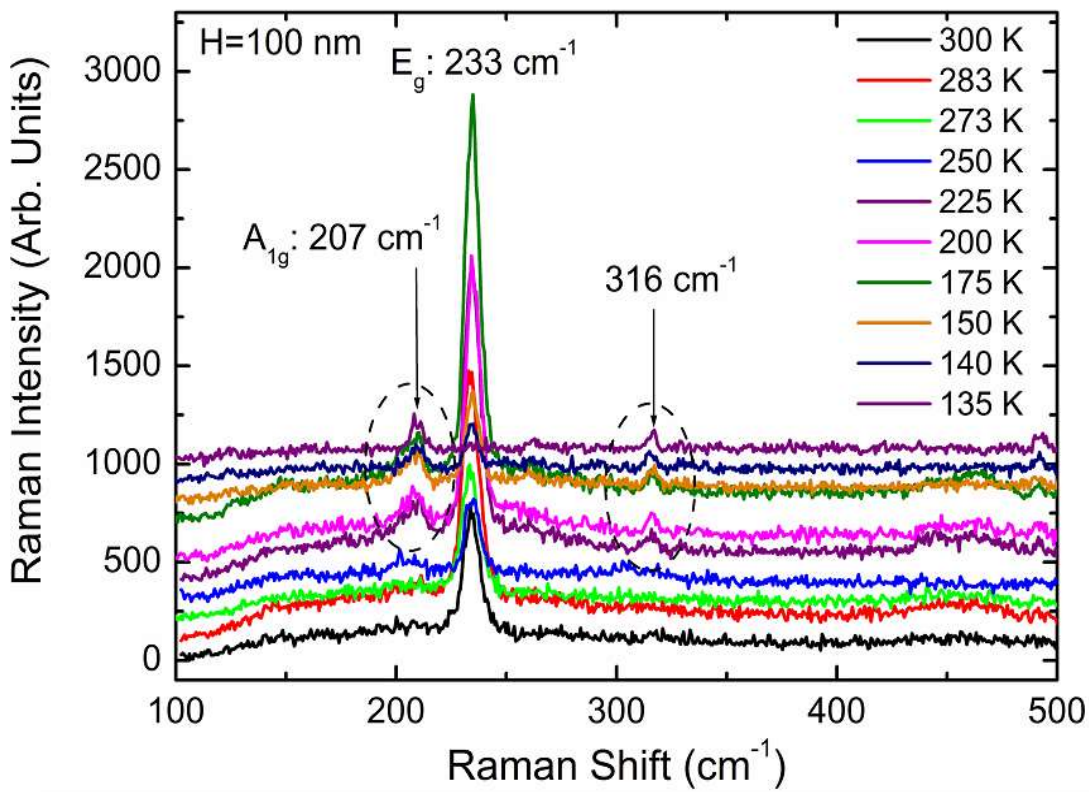

- → Main features are A_{1g} peak at ~207 cm^{-1} and E_g peak at 233 cm^{-1}
- → Peak at 316 cm^{-1} is more pronounced and appears near T_C
- → Temperature at which the spectrum modification is observed is shifter to about ~225 K.
- → Intensity of the low-T Raman peaks varies from sample to sample
- → Emergence of the new Raman lines in $TiSe_2$ is explained by formation of the CDW superlattice below the phase transition temperature

P. Goli, J. Khan, D. Wickramaratne, R.K. Lake and A.A. Balandin, Charge density waves in exfoliated films of van der Waals materials: Evolution of Raman spectrum in $TiSe_2$, Nano Letters, 12, 5941 (2012).

CDW Transition Temperature Scaling with Decreasing Thickness

$TiSe_2$

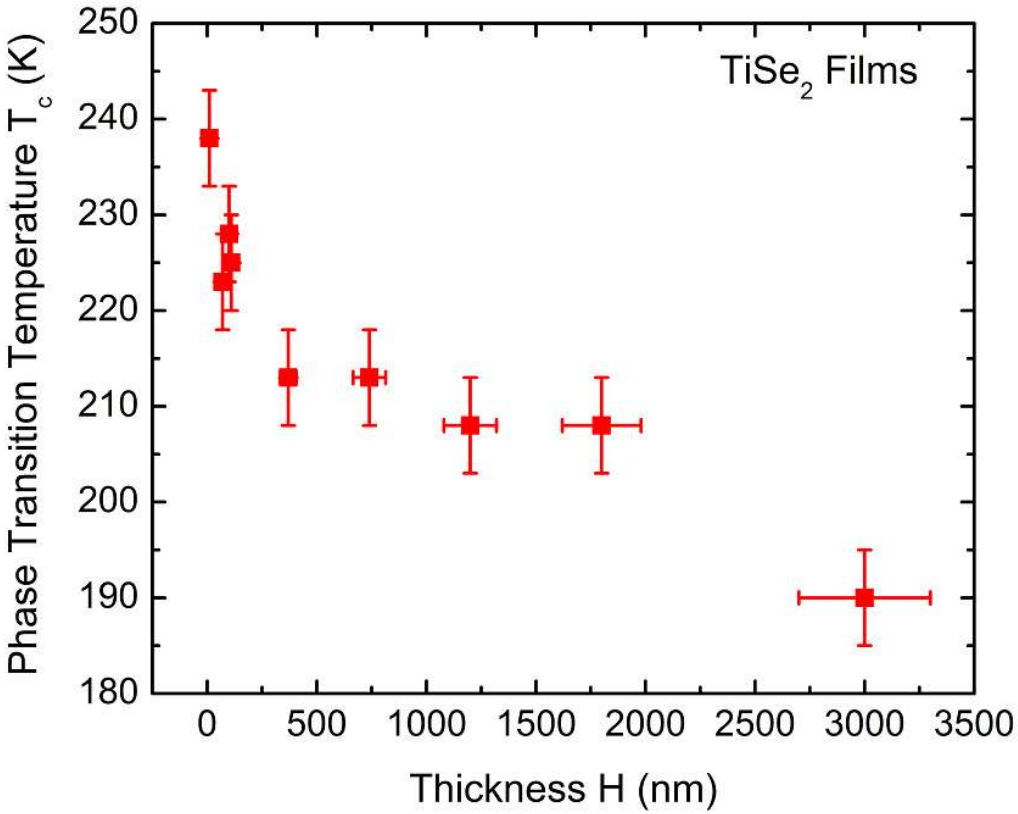

→ CDW transition temperature vs. thickness of the exfoliated $TiSe_2$ thin films.

→ temperature increases from ~200 K in the thick films (H~2 μm) to ~240 K in the thin films (H~100 nm).

→ Major benefit for the proposed electronic applications

Recent theoretical work: M. Calandra, et al., PRB, 80, 241108 (2009)

P. Goli, J. Khan, D. Wickramaratne, R.K. Lake and A.A. Balandin, Charge density waves in exfoliated films of van der Waals materials: Evolution of Raman spectrum in $TiSe_2$, Nano Letters, 12, 5941 (2012).

Collective Current Regime in $TaSe_2$ Channel Devices

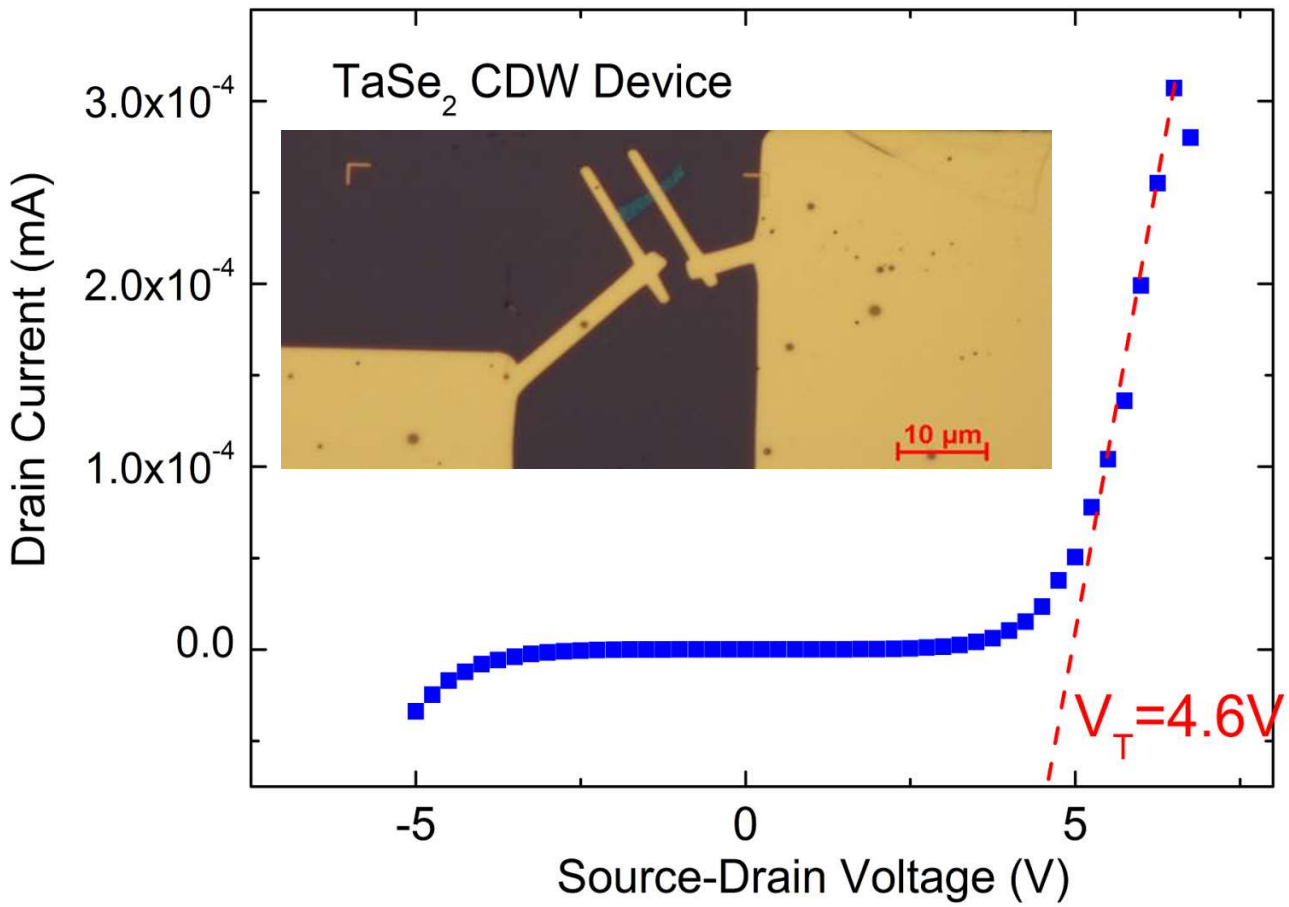

Increase in the apparent threshold voltage is owing to

(i) High concentration of defects
(ii) Size effects
(iii) Possible voltage drop on electrodes
(iv) Channel non-linearity

Part IV: Practical Applications of Phononics

IEEE Spectrum illustration of the thermal issues in the feature article *Chill Out: New Materials and Designs Can Keep Chips Cool* by A.A. Balandin.

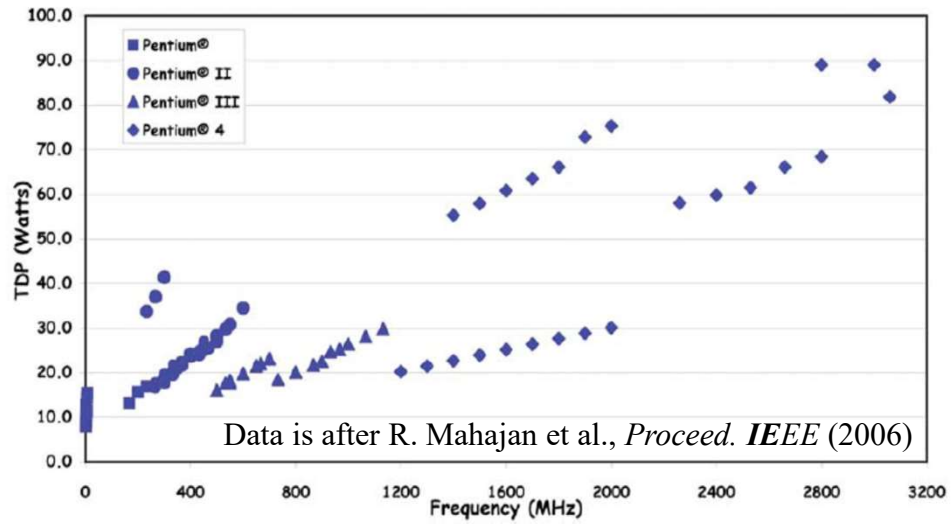

No BIG fan solutions!

→The switch to multi-core designs alleviates the growth in the thermal design power (TDP) increase but does not solve the hot-spot problem

→ Non-uniform power densities leading to hot-spots (>500 W/cm^2)

Increasing Importance of the Thermal Interface Materials - TIMs

TIMs are materials with the relatively high thermal conductivity introduced to the joint to fill the air gaps.

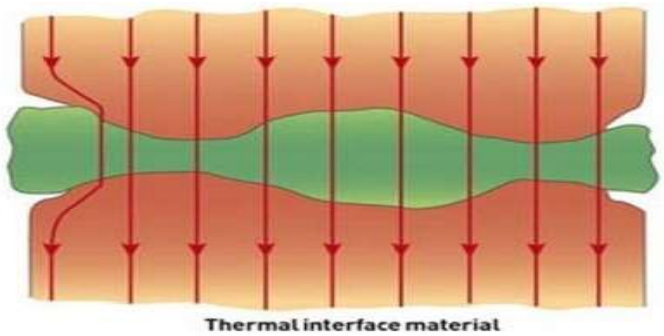

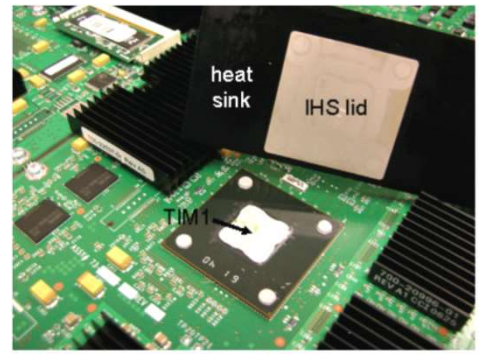

$$R_{effective} = \frac{BLT}{k_{TIM} A} + R_{c_1} + R_{c_2}$$

Current TIM based on polymer, grease filled with silver, alumina require 50-70% loading to achieve 1-5 W/mk.

→ Conventional TIMs: K=1-5 W/mK at the volume fractions *f* of filler ~50% at RT

→ Companies need K=25-30 W/mK

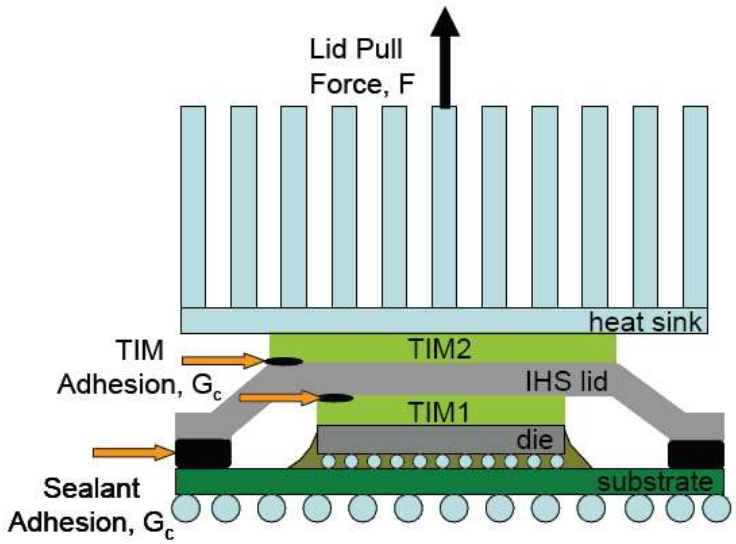

Graphene Enhanced Thermal Interface Materials

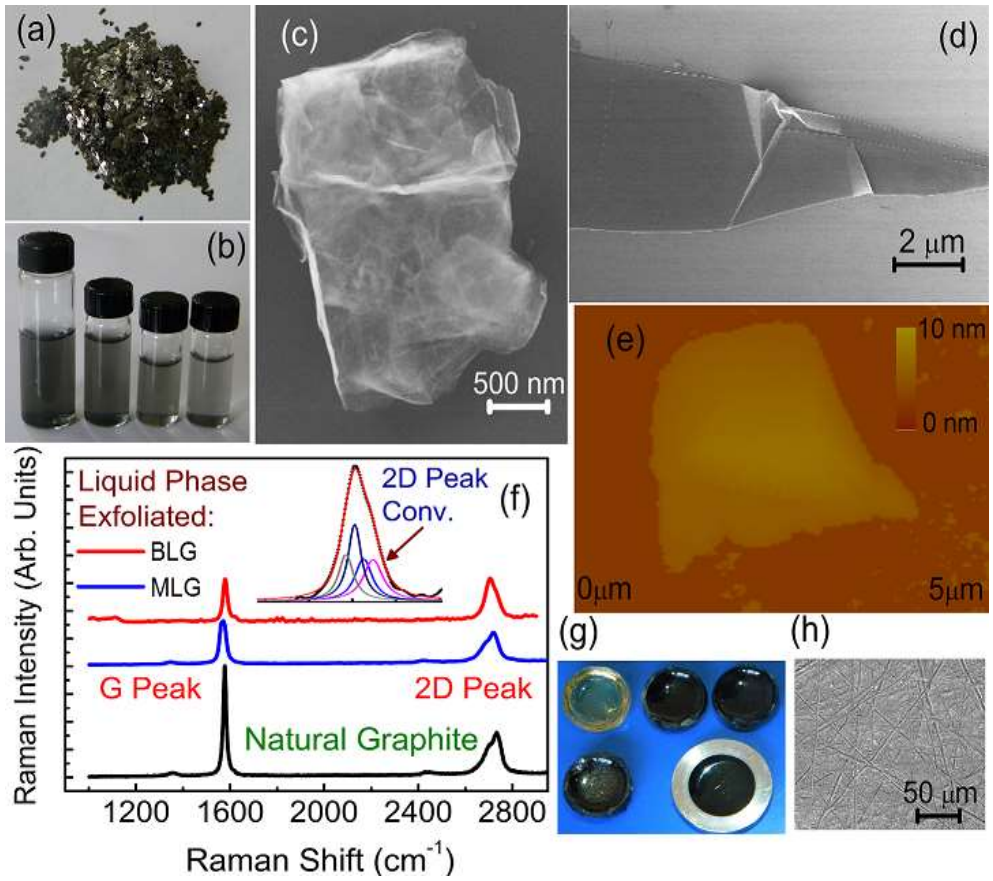

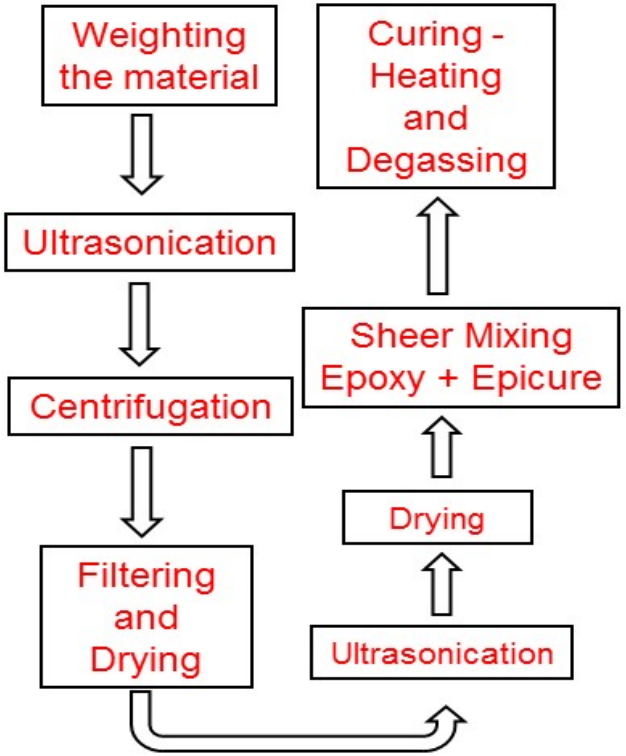

aqueous solution of sodium cholate

K.M.F. Shahil and A.A. Balandin, "Graphene - multilayer graphene nanocomposites as highly efficient thermal interface materials," *Nano Letters*, 12, 861 (2012).

Graphene TIMs with Strongly Enhanced Thermal Conductivity

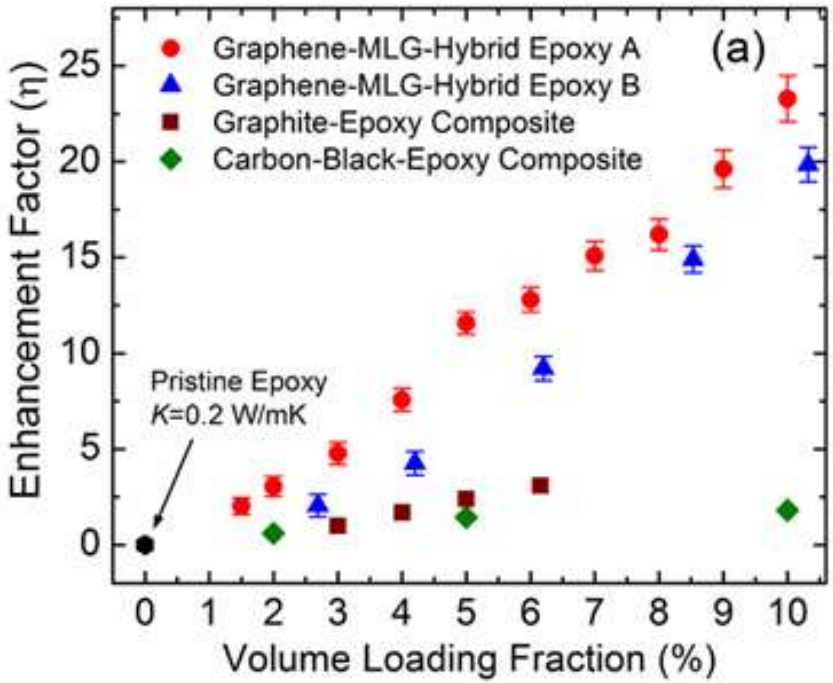

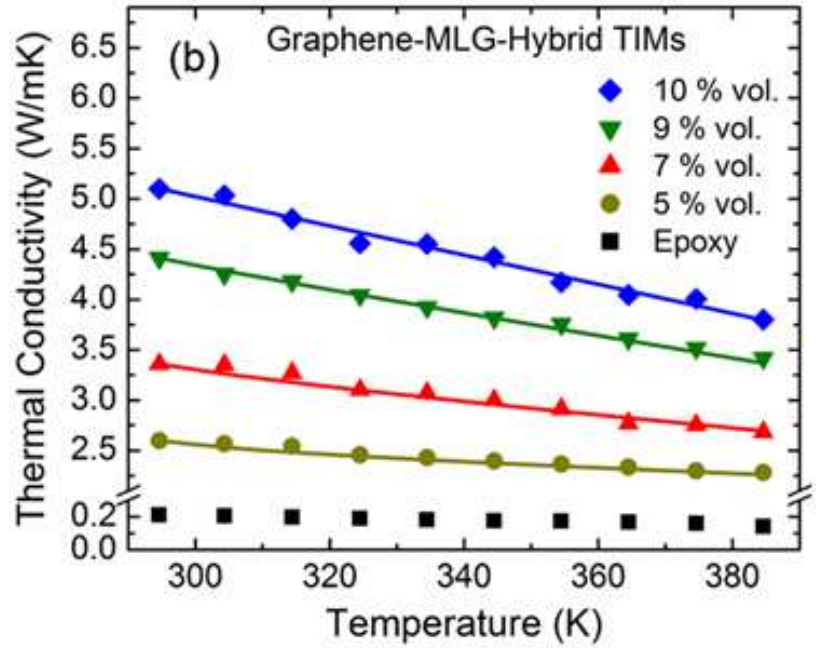

→ Record-high enhancement of *K* by 2300 % in the graphene-polymer at the loading fraction *f* =10 vol.%.

→ K of the commercial thermal grease was increased to K=14 W/mK at the small loading *f*=2 vol. %

K.M.F. Shahil and A.A. Balandin, "Graphene - multilayer graphene nanocomposites as highly efficient thermal interface materials," *Nano Letters*, 12, 861 (2012).

Can Graphene Make PCM Not Only to Store Heat but also to Conduct it Away?

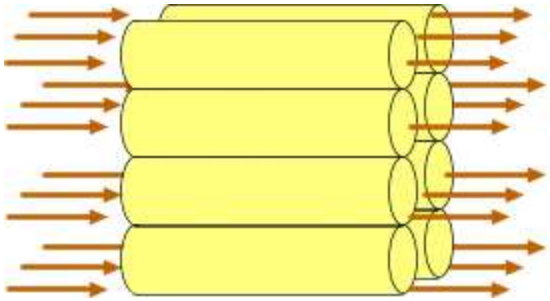

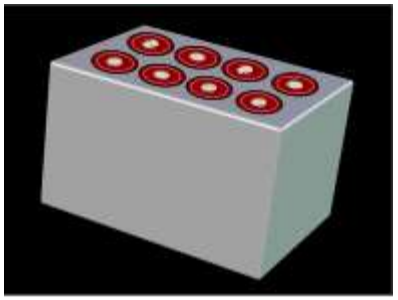

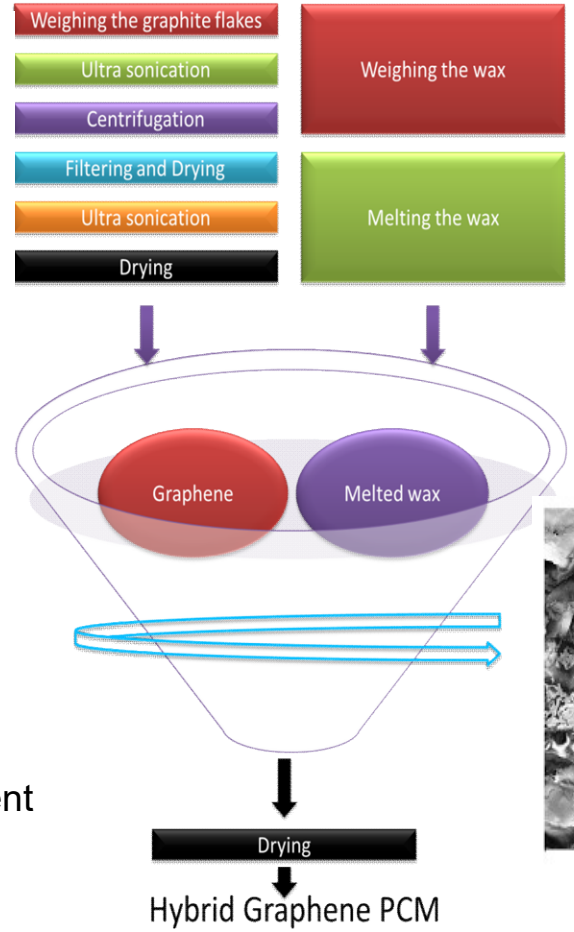

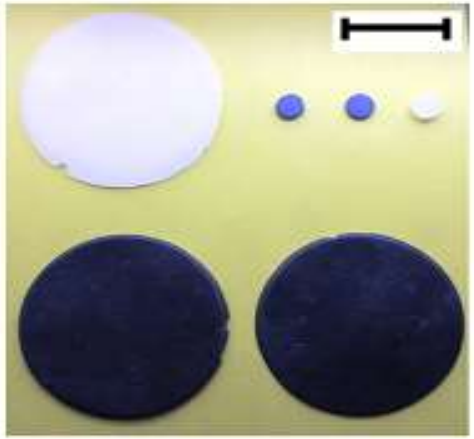

P. Goli, et al., "Graphene-Enhanced Hybrid Phase Change Materials for Thermal Management of Li-Ion Batteries" (2013) – available on arXiv

Hydrocarbon – Graphene Composites as PCMs with Enhanced Thermal Conductivity

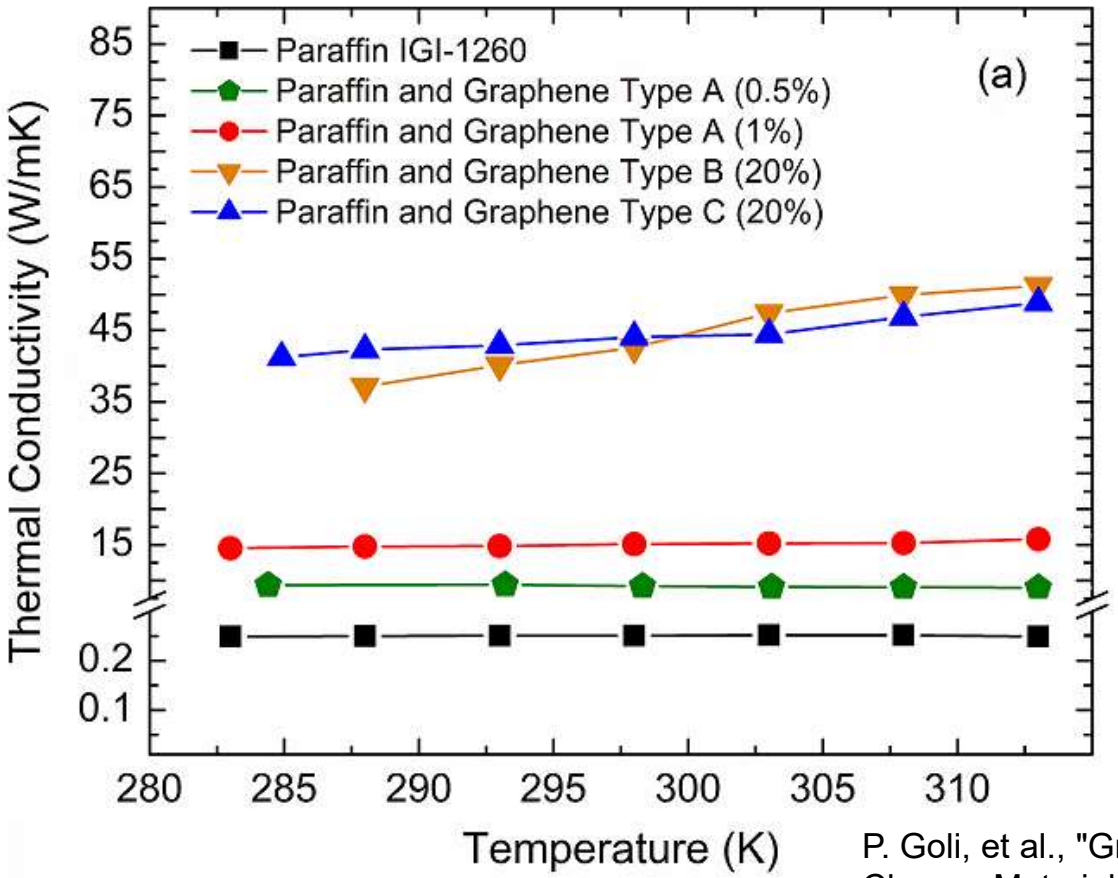

The thermal conductivity enhancement factor, $h=(K-K_m)/K_m$, of about 60 at the 1 wt. % loading fraction is exceptionally high

It is unlikely that uniformly dispersed graphene flakes with a lateral size in the range from 150 to 3000 nm form a thermally percolating network at 1 wt. %

Strongly increased thermal conductivity of the composite is explained by good attachment of hydrocarbon molecules to graphene flakes

P. Goli, et al., "Graphene-Enhanced Hybrid Phase Change Materials for Thermal Management of Li-Ion Batteries," (2013) – available on arXiv.

Testing C_nH_{2n+2} – Graphene Composites for PCM for Battery Thermal Management

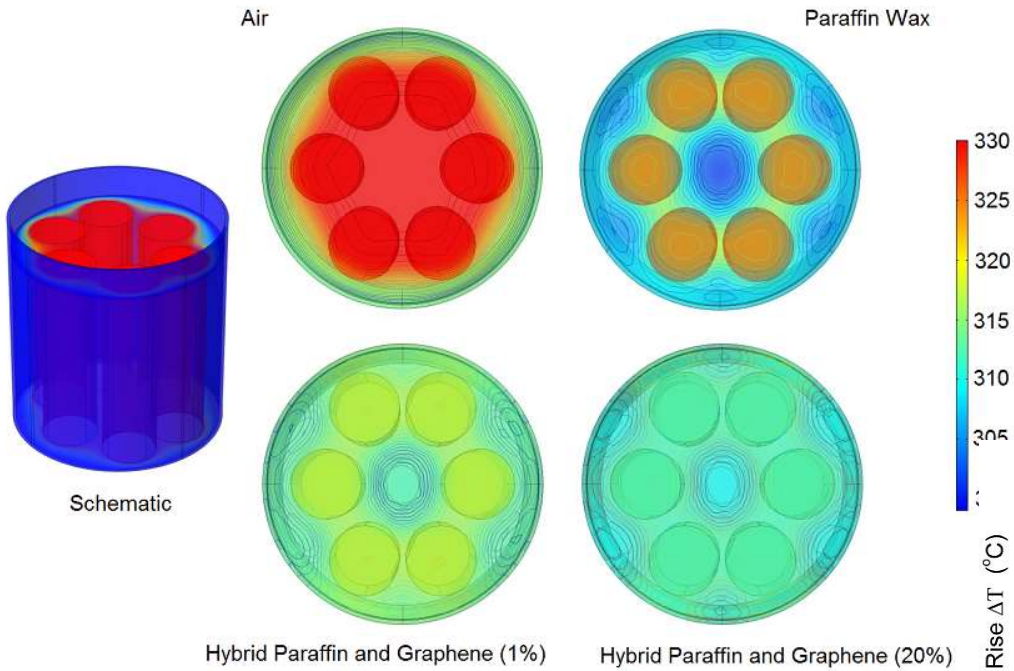

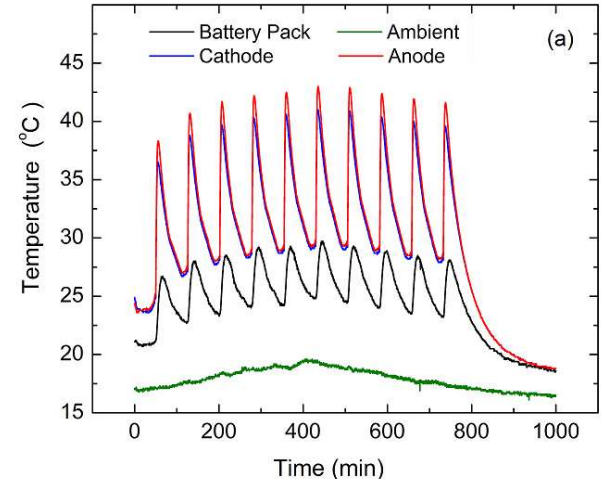

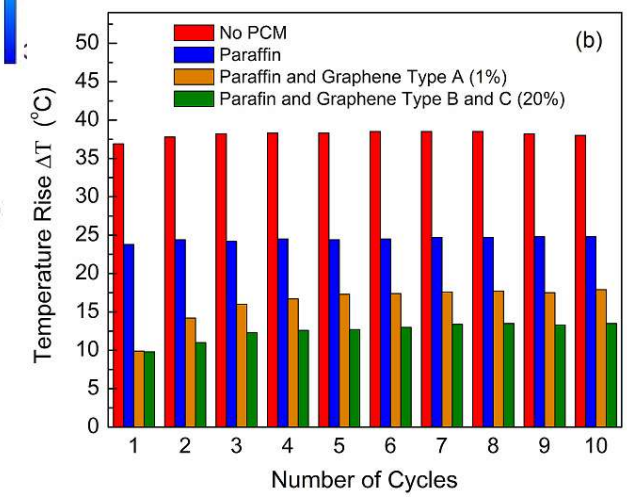

Reduced temperature rise and increased reliability of Li-ion batteries

Graphene *Quilts* for Thermal Management GaN Technology

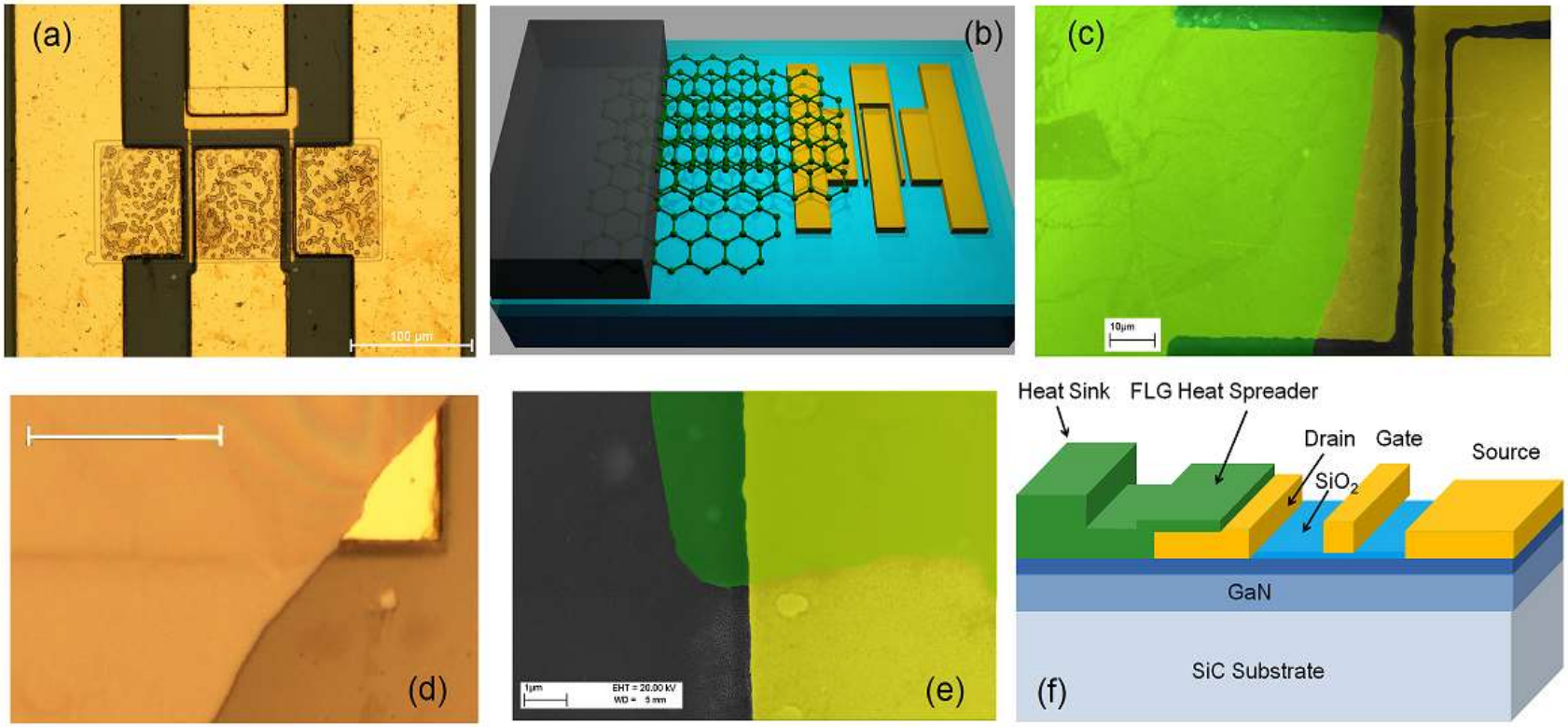

GaN HFETs were used as examples of high-power density transistors; PMMA was utilized as the supporting membrane for graphene transfer to a desired location; the alignment was achieved with the help of a micromanipulator

Z. Yan, G. Liu, J.M. Khan and A.A. Balandin, Graphene-Graphite Quilts for Thermal Management of High-Power Transistors, *Nature Communications* (2012).

Reduction of the Hot-Spot Temperature

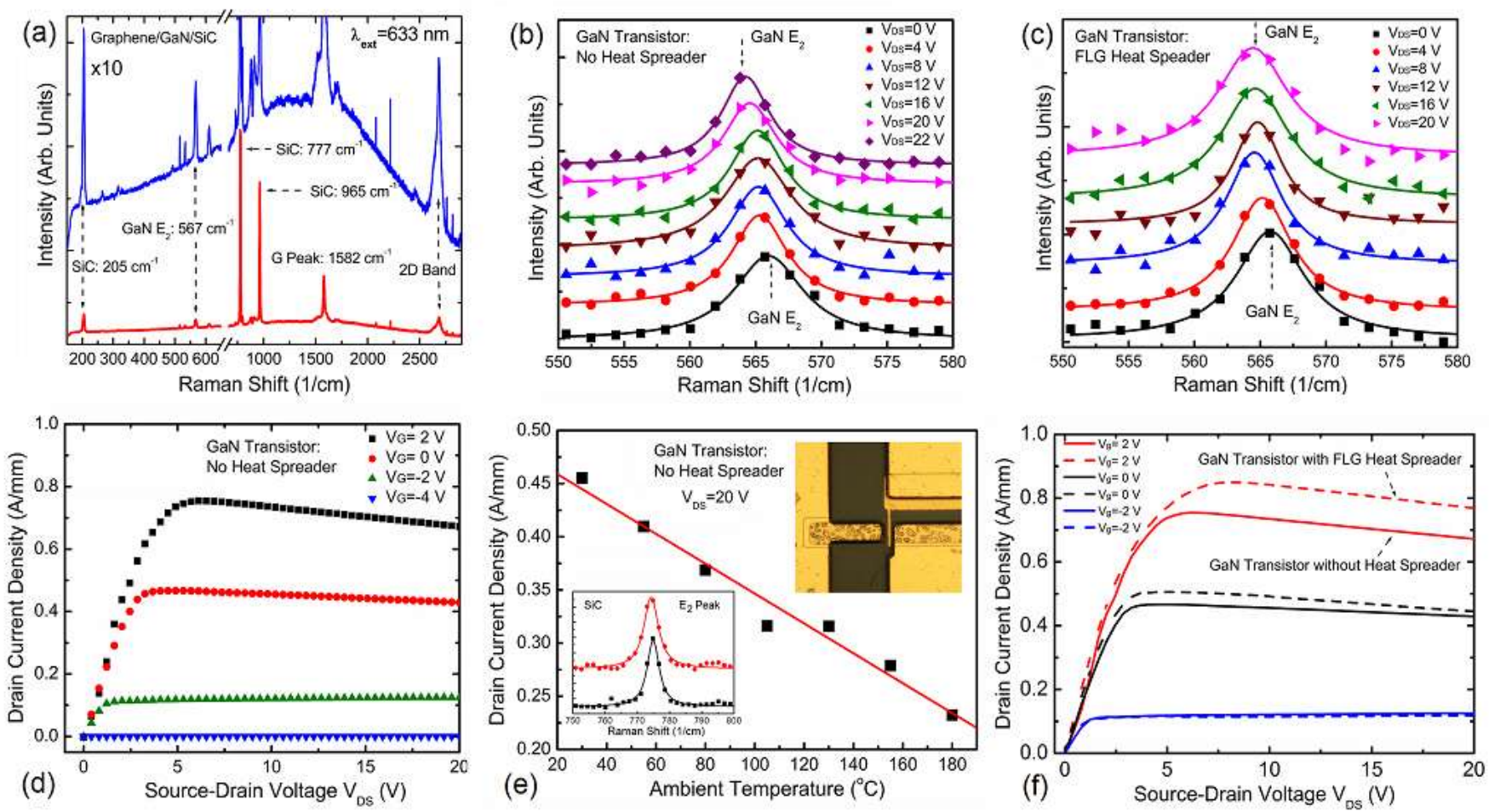

The hot-spots temperature near drain contacts can be lowered by as much as ~ 20°C in such devices operating at ~13-W/mm – translates to an order of magnitude improvement in MTTF

Graphene-on-Diamond – Carbon-on-Carbon Technology

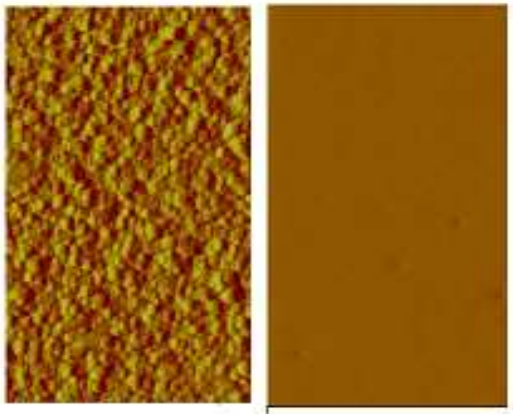

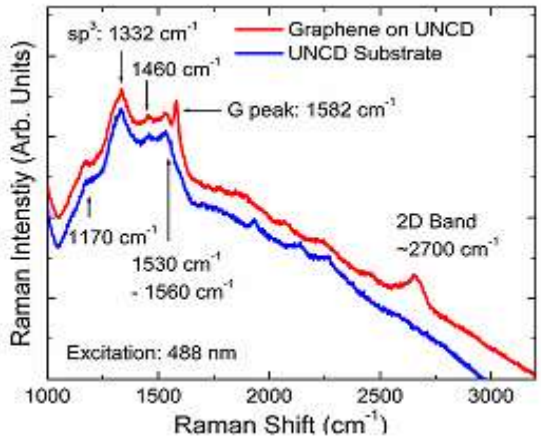

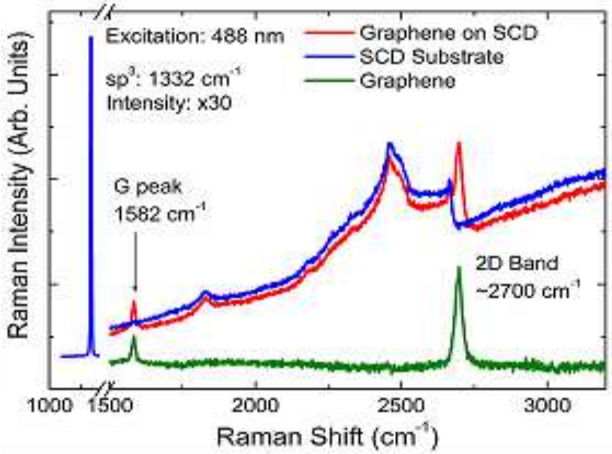

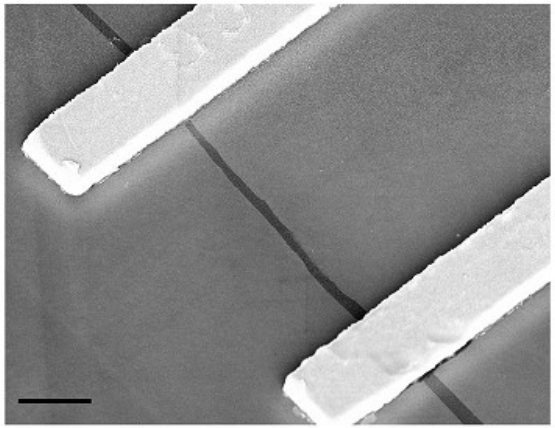

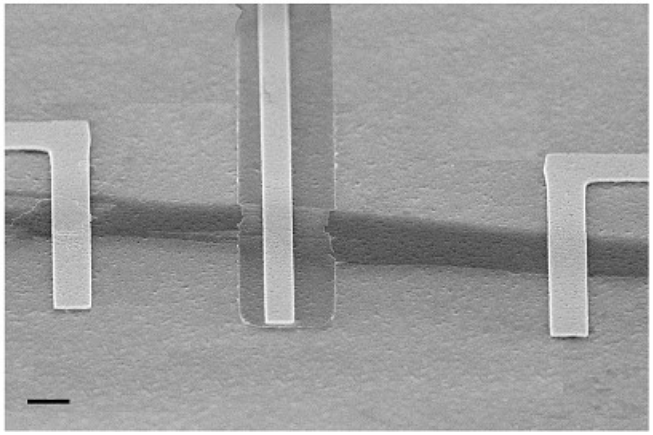

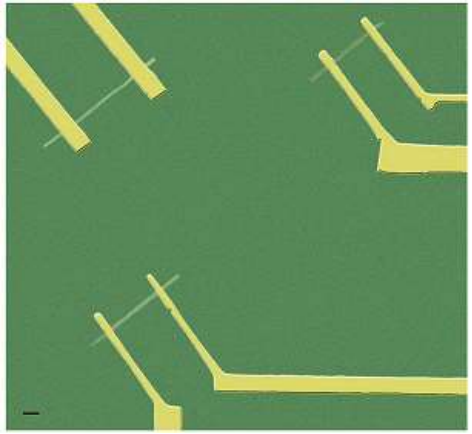

Typical graphene FETs on SiO_2/Si reveal J_{BR} on the order of 10^8 A/cm^2, which is ~100× larger than the limit for the metals but still smaller than the maximum achieved in CNTs

Graphene Interconnects with Extraordinary High Breakdown Current Density

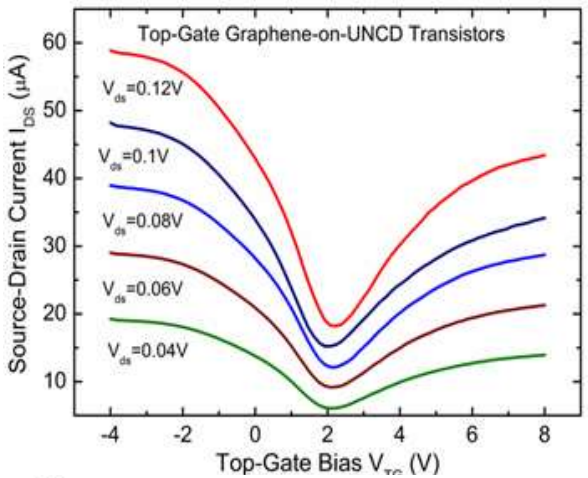

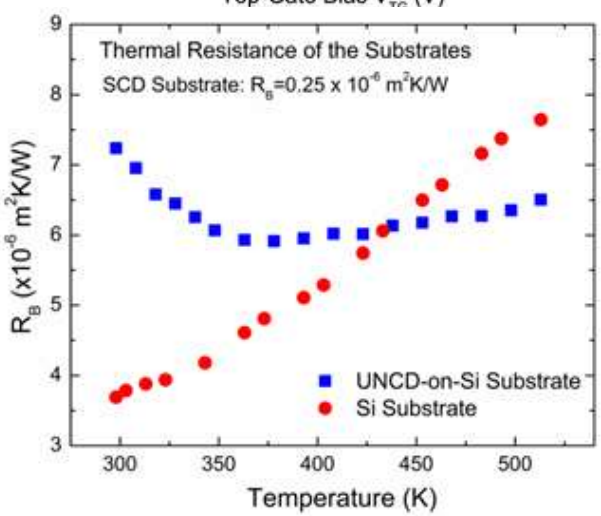

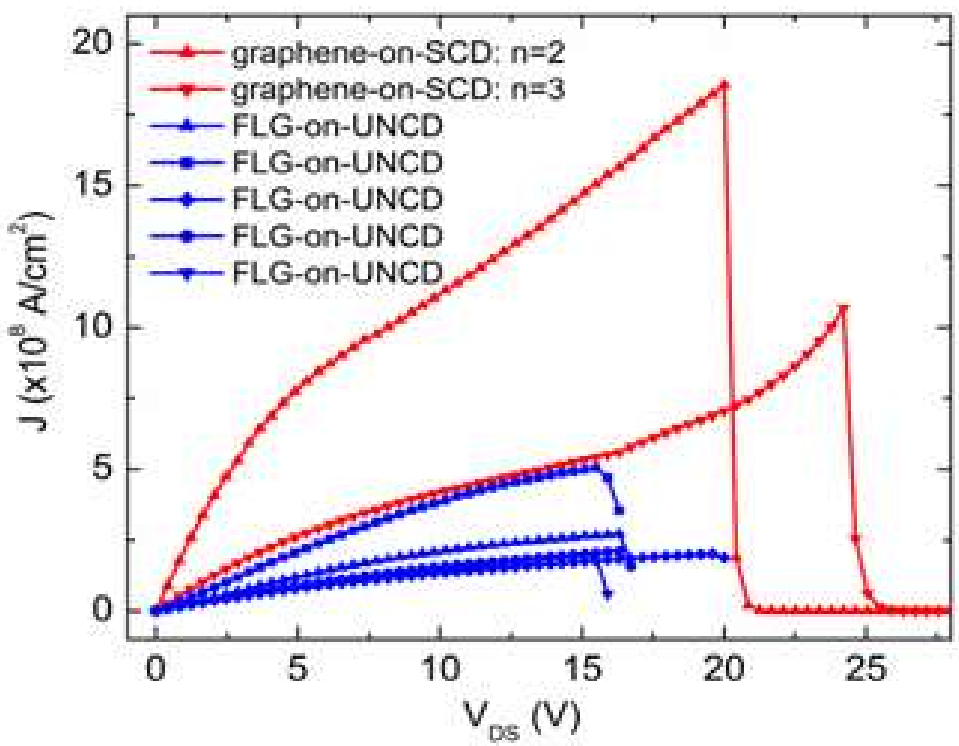

J. Yu, G. Liu, A. Sumant and A.A. Balandin, Graphene-on-diamond devices with increased current-carrying capacity: Carbon sp^2-on-sp^3 technology, *Nano Letters,* 12, 1603 (2012).

Basics of CDW Logic Gates

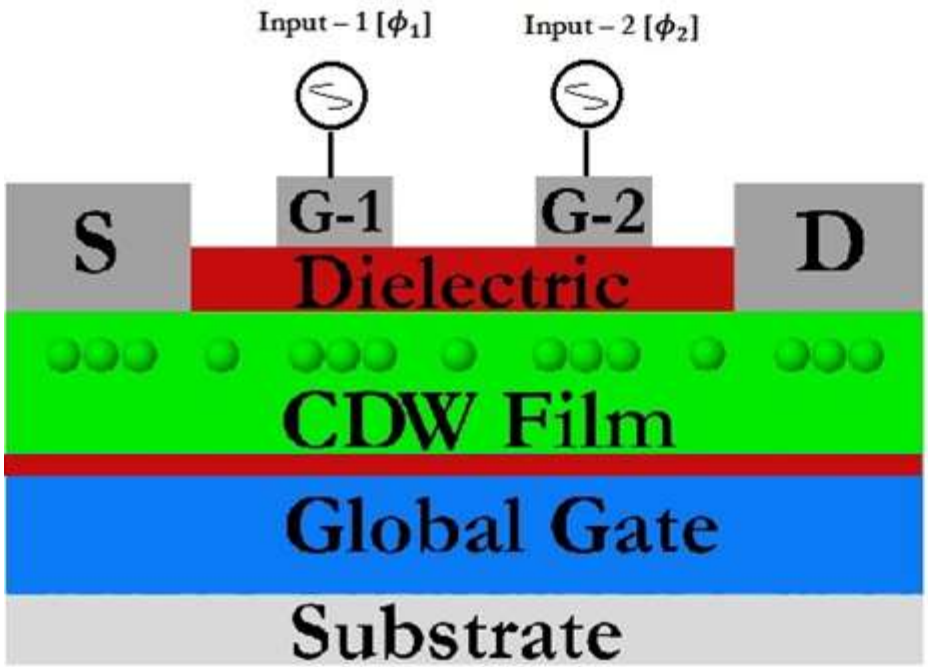

$\phi = 0$ Logic 0

$\phi = \pi$ Logic 1

$V_{in} = 8$ mV

$V_{th} = 9$ mV

Input – 1	Input – 2	Output
0	0	1
0	π	0
π	0	0
π	π	1

$\phi_1 = \phi_2$: constructive interference Output = 1

$\phi_1 \neq \phi_2$: destructive interference Output = 0

Schematic view of the CDW-based EX-NOR gate. Input data is encoded into the phase of the CDW (e.g. $\phi = 0$ corresponds to logic 0, and $\phi = \pi$ corresponds to logic 1). The amplitude of the applied voltage is just below the threshold (e.g. V_{in} = 8 mV; V_{th} = 9 mV). The constructive interference produces CDW of the double amplitude sufficient for de-pinning, which opens the channel. There is no electric current flow in the case of destructive interference.

Practical Motivations for Collective State as Computational State Variables

- Power dissipation became the limiting factor to the continued scaling of size and speed of the CMOS transistors
- If *N* electrons are in a collective state then the minimum dissipation limit for one switching cycle can be reduced from $N k_B T \ln(2)$ to $k_B T \ln(2)$
- Charge density waves (CDW) are collective states, which can exist on a macroscopic scale near room temperature
- CDW can be utilized for Boolean and non-Boolean logic gates and information processing similar to spin waves
- Unconventional materials require innovative techniques for material synthesis and device fabrication

nature materials

REVIEW ARTICLE

PUBLISHED ONLINE: 22 JULY 2011 | DOI: 10.1038/NMAT3064

Thermal properties of graphene and nanostructured carbon materials

Alexander A. Balandin

RT Thermal Conductivity of Carbon Materials:

Diamond: 1000 – 2200 W/mK

Graphite: 20 – 2000 W/mK

DLC: 0.1 – 10 W/mK

***a*-C: 0.01 – 1 W/mK**

NCD-MCD: 1 – 1000 W/mK

CNTs: 1000 – 3500 W/mK

Graphene: 2000 – 5000 W/mK

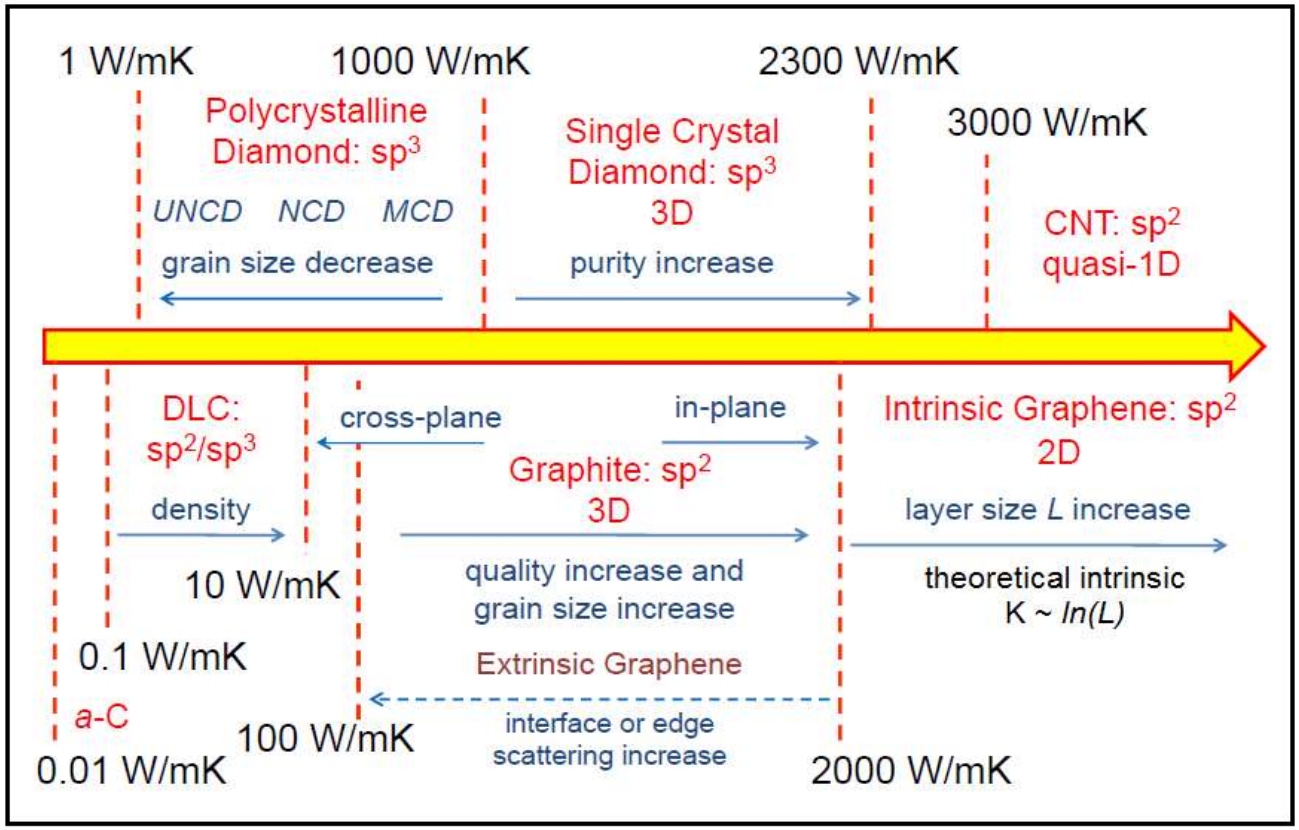

Outlook for Phonon Engineering

- *Phonon confinement effects in nanostructures are observed at room temperature*
- *Nanometer scale is essential for observing and utilizing the phonon confinement effects*
- *Technology has reached the state required for engineering phonon modes*
- *Strong practical motivation due to the problems of heat removal from downscaled computer architectures*
- *Phonon engineering combined with electron band-structure engineering can bring previously unattainable functionality*
- *Graphene and van der Waals materials offer new opportunities for phonon engineering*

| Nano-Device Laboratory >

Acknowledgements

Nano-Device Laboratory (NDL), UC Riverside, 2010 – 2013